



Norwegian University of
Science and Technology

Creating Digital Elevation Model (DEM) based on ground points extracted from classified aerial images obtained from Unmanned Aerial Vehicle (UAV)

Aleksandra Maria Zietara

Master of Science in Civil and Environmental Engineering

Submission date: June 2017

Supervisor: Terje Skogseth, IBM

Norwegian University of Science and Technology
Department of Civil and Environmental Engineering



Report Title: Creating Digital Elevation Model (DEM) based on ground points extracted from classified aerial images obtained from Unmanned Aerial Vehicle (UAV)	Date:		
	Number of pages (incl. appendices): 92		
	Master Thesis	x	Project Work
Name: Aleksandra Zietara			
Professor in charge/supervisor: Terje Skogseth			
Other external professional contacts/supervisors:			

<p>Abstract:</p> <p>With an advent of Unmanned Aerial Vehicles (UAV) and attempts to use them as devices to collect information about terrain, the discussion about the quality of derived products and possibilities of their further use in geomatics applications has begun. One of the desired outputs is the Digital Elevation Model (DEM) which represents the bare-earth surface. To obtain DEM from drone images, the point cloud needs to be filtered in order to remove all the points which are situated above the earth's surface. Most of the available software packages accomplish this with algorithms performing classification on point cloud. Outcomes are often not satisfactory, which results in erroneous DEM.</p> <p>As an alternative solution, the author proposes image classification. The aim of the thesis is to examine the potential of image classification and judge if it could be a satisfying alternative for point cloud classification. Also, the capabilities of consumer-grade drone and drone-dedicated software are going to be evaluated.</p> <p>The first step in the project workflow is capturing data with the use of Phantom 3 Advanced. The photogrammetric flight is prepared having regard to drone specifications, law regulations, and objective of the survey. After the flight, the photos are processed with the use of Agisoft PhotoScan and Pix4D Mapper. Root Mean Square (RMS) for Control Points are 6.12 cm for Pix4D and 7.91 for Agisoft, which are satisfying results. Dense point clouds, DEMs and orthophotomaps are generated and point cloud classification is performed. As the orthophotomap from Pix4D has better resolution (3.36 cm), it is adopted for the process of image classification. This one is performed in ArcGIS Pro software and four classification algorithms are examined in order to choose the best one for this project. The highest accuracy is obtained by Random Trees supervised classifier (76%). Manual improvements are implemented and the map is reclassified into two classes: ground and non-ground objects. Next, the ground class is overlapped with the point cloud and points representing ground are used to generate Digital Elevation Model. DEM obtained from image classification is compared with DEM obtained from point cloud classification. For significant part of the study area the difference is smaller than 0.5 m, but for both models, problematic regions appear in the proximity of buildings and trees.</p> <p>The thesis presents the potential of image classification method and improvements suggested in the last chapter can be adopted for further research of the topic.</p>

Keywords:

- | |
|-----------------------------|
| 1. UAV Photogrammetry |
| 2. Unmanned Aerial Vehicles |
| 3. Digital Elevation Models |
| 4. Image Classification |

MASTER DEGREE THESIS

Course TBA4925 Geomatics, master thesis

Spring 2017

Student:

Aleksandra Maria Zietara

Creating Digital Elevation Model (DEM) based on ground points extracted from classified aerial images obtained from Unmanned Aerial Vehicle (UAV)**BACKGROUND**

Unmanned Aerial Vehicles (UAV) are more and more used in land surveying (geomatics) to obtain Digital Elevation Models (DEM) and other information of the surface of the earth. It is highly wanted to be able to use more automatized processes to obtain a DEM from a point cloud.

TASK

The main goal of this thesis is to look into the possibility of obtaining accurate DEM by using low cost UAV equipment. The focus is on the classification process, by comparing the accuracy and the usability of point cloud classification methods in existing commercial software with each other, and with the image classification method. See the task description below.

Theoretical part

The candidate shall describe and discuss the equipment, the software and the methods used in the thesis: UAV, connection to classical photogrammetry, software packages, DEM, image classification techniques.

Data capture and processing of the captured data

The following instruments and software packages can be used:

GNSS (Leica Viva GNSS GS12), UAV (DJI Phantom 3 Advanced), the software packages Pix4D Mapper, Agisoft PhotoScan, and ArcGIS Pro.

The fieldwork will be done at NTNU campus Dragvoll, where the student shall establish the study field.

Results of the processing of the captured data should be:

Generating Digital Surface and Elevation Models (DSM, DEM), and ortophotomaps from dense point clouds.

Image classifications on ortophotomaps with different classifiers. Separation of ground points and non-ground points, and generating DEMs.

Comparing DEM results with image classification in different software and with different methods.

Results and conclusions

Interpretation, discussion and conclusions of the results achieved, and suggestions of improvements.

STARTUP AND SUBMISSION DEADLINES

Startup: January 15th 2017. Submission date: Digitally in DAIM at the latest June 11th 2017.

SUPERVISORS

Supervisor at NTNU: Terje Skogseth

Co-supervisor: Beata Hejmanowska, AGH University of Science and Technology, Krakow, Poland

Department of Civil and Environmental Engineering, NTNU. Date 15.01.2017 (revised May 2017).

Terje Skogseth (signature)

Abstract

With an advent of Unmanned Aerial Vehicles (UAV) and attempts to use them as devices to collect information about terrain, the discussion about the quality of derived products and possibilities of their further use in geomatics applications has begun. One of the desired outputs is the Digital Elevation Model (DEM) which represents the bare-earth surface. To obtain DEM from drone images, the point cloud needs to be filtered in order to remove all the points which are situated above the earth's surface. Most of the available software packages accomplish this with algorithms performing classification on point cloud. Outcomes are often not satisfactory, which results in erroneous DEM.

As an alternative solution, the author proposes image classification. The aim of the thesis is to examine the potential of image classification and judge if it could be a satisfying alternative for point cloud classification. Also, the capabilities of consumer-grade drone and drone-dedicated software are going to be evaluated.

The first step in the project workflow is capturing data with the use of Phantom 3 Advanced. The photogrammetric flight is prepared having regard to drone specifications, law regulations, and objective of the survey. After the flight, the photos are processed with the use of Agisoft PhotoScan and Pix4D Mapper. Root Mean Square (RMS) for Control Points are 6.12 cm for Pix4D and 7.91 for Agisoft, which are satisfying results. Dense point clouds, DEMs and orthophotomaps are generated and point cloud classification is performed. As the orthophotomap from Pix4D has better resolution (3.36 cm), it is adopted for the process of image classification. This one is performed in ArcGIS Pro software and four classification algorithms are examined in order to choose the best one for this project. The highest accuracy is obtained by Random Trees supervised classifier (76%). Manual improvements are implemented and the map is reclassified into two classes: ground and non-ground objects. Next, the ground class is overlapped with the point cloud and points representing ground are used to generate Digital Elevation Model. DEM obtained from image classification is compared with DEM obtained from point cloud classification. For significant part of the study area the difference is smaller than 0.5 m, but for both models, problematic regions appear in the proximity of buildings and trees.

The thesis presents the potential of image classification method and improvements suggested in the last chapter can be adopted for further research of the topic.

Acknowledgments

I would like to express my sincere gratitude to Terje Skogseth who was the supervisor and provided me with an opportunity to accomplish the thesis. I would like to thank him for his time, support and priceless guidance.

I am grateful to my Polish supervisor, Beata Hejmanowska, for all her invested time, assistance and encouragement to reach the goal.

I am also grateful to my cousin Faustyna Zietara who lives in Canada and offers me writing assistance and language editing.

Abbreviations

BLOS	Beyond Line of Sight
CP	Check Points
DEM	Digital Elevation Model
DSM	Digital Surface Model
DTM	Digital Terrain Model
EUREF 89	European Reference Frame 1989
EXIF	Exchangeable Image File Format
GCP	Ground Control Points
GIS	Geographic Information System
GNSS	Global Navigation Satellite System
GPS	Global Positioning System
GSD	Ground Sample Distance
IMU	Inertial Measuring Unit
INS	Inertial Navigation System
LiDAR	Light Detection and Ranging
ML	Maximum Likelihood
NVDI	Normalized Difference Vegetatio Index
PH3A	Phantom 3 Advanced
RMS	Root Mean Square
RPA	Remotely Piloted Aircraft
RPV	Remotely Piloted Vehicle
RT	Random Trees
RTK	Real Time Kinematics
SfM	Structure from Motion
SVM	Support Vector Machines
TIN	Triangular Irregular Network
UAS	Unmanned Aircraft System
UAV	Unmanned Aerial Vehicle
UTM	Universal Transverse Mercator
UVS	Unmanned Vehicle Systems
VLOS	Visual Line of Sight

Table of contents

Abbreviations	iii
1 INTRODUCTION.....	1
1.1 Thesis objectives.....	2
1.2 Outline of thesis.....	2
2 THEORETICAL BACKGROUND	4
2.1 UAV Platforms	4
2.1.1 Applications	5
2.1.2 Classification.....	6
2.1.3 Flight regulations.....	7
2.1.4 Benefits and drawbacks.....	8
2.1.5 Phantom 3 Advanced	9
2.2 UAV Photogrammetry.....	11
2.2.1 Flight plan	13
2.2.2 Post processing.....	14
2.2.3 Ground Control Points	15
2.3 Digital Elevation Model	16
2.3.1 Applications	18
2.3.2 Acquisition	18
2.4 Image Classification	19
2.4.1 Image classification algorithms.....	21
2.4.2 Accuracy assessment.....	22
2.5 Software.....	24
2.5.1 Agisoft PhotoScan.....	25
2.5.2 Pix4D Mapper	25
2.5.3 ArcGIS Pro.....	26
3 PROJECT WORKFLOW	27
3.1 Study area and ground control points	27

3.2	Image acquisition.....	29
3.2.1	Flight planning	29
3.2.2	Flight	32
3.3	Image processing	32
3.3.1	Agisoft PhotoScan.....	34
3.3.2	Pix4D Mapper	35
3.3.3	Accuracy Assesment	37
3.3.4	Point cloud classification	39
3.4	Image classification	41
3.4.1	Data preparation	41
3.4.2	Classification process.....	43
3.4.3	Accuracy assessment.....	48
3.4.4	Post-classification processing	54
3.5	DEM generation	56
4	DISCUSSION AND CONCLUSIONS.....	61
	Bibliography.....	65
	List of figures	68
	List of tables	69
	Appendices	70

1 INTRODUCTION

In the recent years, Unmanned Aerial Vehicles have undergone rapid expansion. They play a great role in a variety of fields. They also find an application in land surveying as a device to measure the ground. With the use of fundamental rules of photogrammetry, drones are used to investigate the surface of the earth. Due to very high spatial resolution of the photos acquired from UAV's, aerial surveys are becoming increasingly popular. Drones seem to be more effective than ground surveys with the use of total station in the small areas of investigation, and their cost effective compared to aerial flights with the photogrammetric camera mounted on the board. But the main concern remains – are the aerial surveys carried out by UAV accurate enough to be used in engineering applications? Over recent years, many investigations have been done to evaluate the quality of products generated from data collected by drones. For instance, Okamoto (Okamoto & Shimazaki, 2015) examined if UAV can be a substitute for conventional terrestrial surveying methods, while (Madawalagama, et al., 2016) provided the assessment of accuracy among survey-grade and consumer-grade drones. Some researchers have also been focused on Digital Elevation Model generation from images obtained from drone (Uysal, et al., 2015). Most of the studies resulted in a positive picture of drones and its usage in geomatics applications.

With a growth in a number of UAV surveys applications, the number of drone dedicated software available on the market increasing as well. Some of the examples are commercial Pix4D and Agisoft PhotoScan. Despite the fact that programs of this type allow generating a dense 3D point cloud, Digital Surface Model, and georeferenced orthophotomap, follow a different workflow. Sona (Sona, et al., 2014) compared Pix4D and Agisoft PhotoScan in order to evaluate their effectiveness and weaknesses. Their studies were focused on the differences between final products generated by different software such as Root Mean Square (RMS) of standard deviation, RMS of the control points and DSM comparison.

1.1 Thesis objectives

The aim of the investigation is to evaluate the accuracy of Digital Elevation Model generated from aerial imagery obtained with the use of Unmanned Aerial Vehicles. Multiple factors including of factors such as overlapping, flight altitude, camera resolution and, deviations of GPS/INS devices which affect the final accuracy of the model and have already been subject to investigation (Ruiz, et al., 2014). However, the main concern of this thesis is to find the answer if the workflow of the mentioned software is sufficient in terms of generating accurate and reliable DEM only from bare-Earth points. Since UAV-based point clouds are not capable of viewing beneath the forest canopy and do not represent the topography of the bare earth surface as successfully as Light Detection and Ranging method (LiDAR), filtering UAV-based point clouds is more challenging (Yilmaz, et al., 2016). General approach is to start from DSM, analyse and eliminate object surfaces and finally generate DEM. As the available software filter point cloud almost completely automatically, the image classification is implemented as a separate process. It will allow for the comparison of different methods while validating, which of them provides the most satisfying results.

1.2 Outline of thesis

The fundamental objective of the project is to examine the potential of image classification technique adopted as one of the stages of post-processing images obtained from a drone. As the workflow requires many separate steps, the structure of the thesis is complex and comprises many subsections inside four main chapters.

Chapter one is an introduction and serves as an explanation of the topic. It refers to literature and describes previous investigations based on akin subject. The chapter also outlines the main assumptions and objectives of the thesis.

Chapter two contains all theory related to the subject of the project. Review of the literature combined with author's knowledge and experiences serves to guide in the description of the topics raised in the thesis. UAV platforms and UAV photogrammetry sections contain essential information related to the appearance of drones in geomatics field. The content starts the with description of the drones, containing their applications and discussion about advantages and limitations. Next, the differences between UAV and classical photogrammetry are expounded and details of flight planning and processing drone images are characterized. The following sections deliver a brief description of Digital Elevation

Models and image classification techniques. The overview of different classification algorithms is introduced and accuracy assessment methods are demonstrated. In the last subsection of the first chapter, software packages adopted in the project with their specifications are presented.

Chapter three is the fundamental part of the thesis as it describes the practical approach to accomplish its objectives. It starts with a presentation of the study area, followed by the description of image acquisition process. Both flight planning assumptions and flight procedures are characterized. The next section focuses on drone images processing performed in Agisoft PhotoScan and Pix4D Mapper. It ends with the comparison of two software packages assisted by accuracy assessment and illustrates the unsatisfying results of the point cloud classification process.

The fourth section demonstrates the complex process of image classification, comprising all of the challenges and attempts to obtain satisfactory outcomes. In post-classifying processing, the point cloud that covers the whole area of study is clipped with classified raster in order to remove all points which present non-ground objects. The last section of practical part of the thesis describes the DEM generation process and finally allows for the comparison of two point clouds acquired with different approaches: one created in a process of point cloud classification and the other one created in the process of image classification. As the workflow of the thesis requires analysing some results before moving to next steps, some comments and author's observations are also included in this chapter.

The last chapter contains a summary of the previous sections followed by results interpretation. What is more, the discussion and conclusions related to all the topics raised in the project are included. Due to the research nature of the thesis where the potential of proposed solution was examined, the last chapter also contains a list of challenges and improvements for the future studies.

2 THEORETICAL BACKGROUND

This chapter is a theoretical part of the thesis. It is divided into five sections covering different topics which are part of the project. Also, an overview of literature is included in following subchapters. Section one describes key aspects of UAV platforms that include their applications, classification, low regulations, drawback and benefits, and also specifications of Phantom 3 Advanced. In section two, UAV photogrammetry as a new technology is presented and comparison with classical photogrammetry is provided. Flight planning, image processing, and Ground Control Points measurements are described with regard to imagery from drones. What is more, the assumptions required for capturing data in practical part of the thesis are introduced. Section three contains characteristics of DEM including its acquisition and applications. A difference between Digital Elevation Model and Digital Surface Model is explained and LiDAR technology as the main source of capturing height data for extension areas is described. The fourth chapter focuses on image classification process. It starts with a general overview followed by characteristics of different classification algorithms and presentation of confusion matrix which is one of the accuracy assessment methods. The main objective of the fifth chapter is an introduction to software packages used in the project. A brief description of Agisoft PhotoScan, Pix4D Mapper and ArcGIS Pro and their specifications is included.

2.1 UAV Platforms

The Unmanned Aerial Vehicle is stated to be the aircraft designed to operate without a human on the board. It can be piloted by remote control, can fly autonomously or semi-autonomously. The term UAV is the most popular term but not the only one found in the literature. Other terms include Unmanned Vehicle Systems (UVS), Unmanned Aircraft System (UAS), Remotely Piloted Aircraft (RPA), Remotely Piloted Vehicle (RPV) and drone. These terms have similar meanings and could be used interchangeably (Eisenbeib, 2009).

Unmanned Aerial System consists of three components: an aircraft, flight control system and ground control station. The aircraft equipped with Inertial Measuring System (IMU) and Global Navigation Satellite System (GNSS) is connected to the ground control

station via telemetry. It allows the operator to control the flight, monitor the camera view and have insight into flight parameters such as flight altitude, remaining time flight, aircraft position and status. Different flight modes serve for different purposes. In a manual mode, a drone operator has full control over the aircraft. Semi-autonomous mode compensates the influence of the wind, as a GNSS receiver is responsible for keeping the drone in its exact place. It makes piloting the drone easier, but is elusive in areas with many electronic devices, which could influence the GNSS receiver. The most common mode in photogrammetric flights is autonomous mode. The drone flight path is then predefined and the aircraft follows a path of waypoints, which are points with determined xy coordinates and altitude.

2.1.1 Applications

The advent of drones has its roots in military purposes. There was a need to invent aircraft which could penetrate hostile terrain without the deployment of human beings in areas of high risk (Eisenbeiss, 2004). With time, society noticed the potential of UAV and started to develop, regulate and apply this technology for commercial purposes. Nowadays, the application of drones is found in many different fields.

One of the most popular is aerial photography which enriches services of photographic companies. Photos from drones are used in advertisements, movies while many mass cultural or sporting events can be captured from UAV's. It also attracts many travellers and non-commercial users to present their adventures from a different view, so the internet is full of outsized records from drones.

Agriculture and forestry are other sectors in which deploying drones is practical and beneficial. UAV platforms equipped with multispectral cameras create photographs in visible and infrared portions of spectrum which allows for the monitoring of vegetation and computing the Normalized Difference Vegetation Index (NDVI). NDVI is an indicator used in remote sensing measurements which allows to assess the condition of vegetation by detecting how green the leaves are. With the use of drones, this index can be determined for large areas in a short time allowing for proper actions to be undertaken.

Unmanned Aerial Vehicles have also been adopted in search and rescue operations and disaster mapping. Due to their small size and resistance to some environmental factors (such as temperatures or chemical substations), drones are useful in search campaigns in areas inaccessible by humans. Periodic inspections could also prevent disasters such as landslides and creeks. In addition, flying a drone over areas damaged by tornado, flood or volcano

eruption provides accurate imaging of the degree of devastation. These images can assist in the creation and implementation of post-disaster rescue plans.

What is more, drones were revolutionary in the geomatics field. New terminology such as *UAV photogrammetry* has been introduced (Eisenbeib, 2009), which could be understood as a new photogrammetric measurement tool. Drones are cost friendly and allow for the capture of photos in a short time which attracts many surveying companies. Obtained in post processing products such as orthophoto maps, Digital Elevation Models and 3D point cloud models are source of valuable information. There are many studies underway that examine if these small aerial vehicles can replace traditional photogrammetry and ground surveying and if so, then to which extent can it be done.

These are only some examples of drones' usage. Drones are also deployed in 2D and 3D mapping in order to support environmental surveys, archaeology, inspections and surveillance. The common and fundamental target of the fields mentioned above is gathering information with the use of the drone. What differentiate them is analysing data in a way suitable for specific purpose and consequently processing, generating and implementing output products.

2.1.2 Classification

Many Civil Aviation Authorities established classification schemes specific to their countries. There are no universal or official approaches, they vary with region and law regulations. A great number of factors could determine classification rules. The most general categorization is the shape and construction of the aircraft vehicle. Two very common types in UAV photogrammetry could be distinguished: fixed wing aircrafts (Fig. 1.a) and multi-rotors (Fig. 1.b). Fixed wing aircrafts seemed to be more powerful, with long flight duration time and better stability. On the other hand, they are not capable of staying in one position, take off or land in a vertical line. Due to their lower cost, most of the non-commercial drones are multi-rotors. Other ways of the division might depend on weight, size, and payload of the drone. Aerial vehicles range from very small weighting less than 1kg, to complex and more sophisticated systems, over 150 kg with payload mass allowing them to lift professional cameras. The flight duration time, range and flight altitude could also be a base to form division scheme.

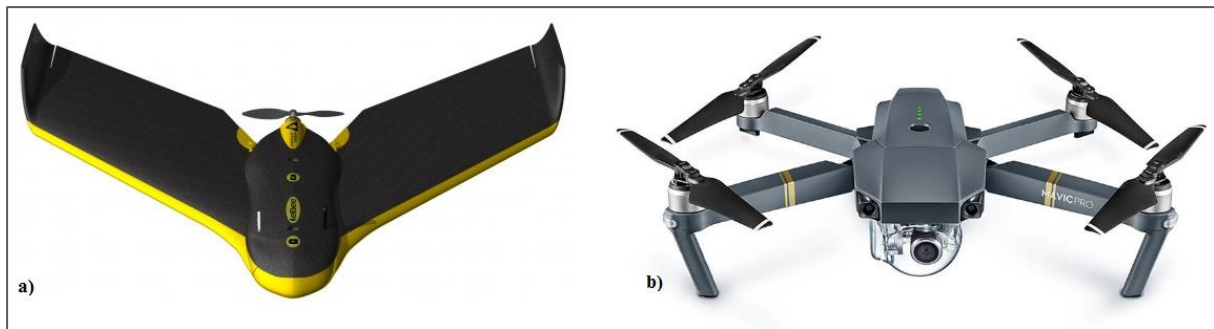


Figure 1 On the left: fixed wing eBee SenseFly, On the right: rotary wing Mavic DJI
Source: www.sensefly.com, www.dji.com

2.1.3 Flight regulations

Recently, the use of UAV has become so popular that they are accessible to everyone. Drones have even become toys for both children and adults. As a result, a serious concern has appeared – the safety. Drone related occur frequently due to two main reasons. One of the reasons is human factor, such as lack of danger awareness. The other reason is the imperfect nature of drones as machines. To reduce the number of disasters, Civil Aviation Authorities from many countries introduced rules and regulations, which should be respected by certified UAV operators but also by people who use drones for entertainment. Considering Norwegian Civil Aviation Authority, the Aviation Act (*Lov of luftfart, Forskrift om luftfartøy som ikke har fører om bord mv.*) is legal act obligatory in Norway. The main rules for inhabitants are as follows:

- Flights closer than 5km to the airport are forbidden,
- Drones must be in a light of sight, no higher than 120 m above a ground,
- A distance of 150 m from people, buildings, and traffic must be kept,
- Drones must be operated in a mindful and considerate manner,
- Full responsibility of damages to people and property is taken by the drone operator.

As a comparison, Polish Civil Aviation Authority's rules are also cited. There are some acts which regulate drone practice ¹ and the main assumptions can be defined:

- Flight must be performed in a line of sight,

¹ Ustawa z dnia 3 lipca 2002 r. Prawo Lotnicze, Rozporządzenie Ministra Infrastruktury I Budownictwa z dnia 8 sierpnia 2016 r. zmieniające rozporządzenie w sprawie wyłączenie zastosowania niektórych przepisów ustawy – Prawo lotnicze do niektórych rodzajów statków powietrznych oraz określenia warunków i wymagań dotyczących używania tych statków, Rozporządzenie Ministra Infrastruktury i Budownictwa z dnia 19 września 2016 r. zmieniające rozporządzenie w sprawie świadectw kwalifikacji

- One shouldn't fly above people, buildings, and roads,
- The drone operator takes full responsibility for a flight which should be performed in a safe and considerable manner,
- Flights closer than 6km to the airport are forbidden
- The drone operator should consider weather conditions (such as strong wind, rain or solar storm) and terrain obstacles.

Presented rules refer to all citizens and their task is to advise non-commercial users not to fly carelessly. Nevertheless, legislations contain more regulations which describe airspace, limitations of flights in different zones, possible methods of flight such as Visual Line of Sight (VLOS) or Beyond line of sight (BLOS) and types of aircrafts. There are also rules that mainly apply to certified drone operators, which describe the procedure of examination, requirements, and tasks for pilots. Aviation Personnel Certificate of Qualifications is required in both Poland and Norway in order to perform commercial flights. One of the conditions in obtaining the certificate is to pass the state examination, which contains questions about airspace, unmanned aerial vehicles, law regulations and first aid.

The intention of this chapter was to present that each photogrammetric flight should meet the requirements, the pilot should know the structure and limitations of the aircraft and the drone should be operated in a thoughtful and careful manner.

2.1.4 Benefits and drawbacks

UAV photogrammetry is considered to be a low-cost alternative to the classical aerial photogrammetry. The main advantage is the price of the vehicle, reduction of operational costs but also the accessibility and real-time capability of data acquisition, transmission, and processing. Most of the drones are equipped with IMU and GNSS navigation systems which allow for mission planning and can obtain preliminary coordinates of the centre of images. Known parameters of photos external orientation reduce the processing time required for a software to perform feature matching and block adjustment. Another thing to consider is the weather. In many places across the world, photogrammetric missions can be performed only during few days in a year due to cloudy skies and fog. Drones are capable of capturing photos from low altitudes, allowing the vehicle to operate from beneath the clouds, which significantly increases the number of possibilities of when the flight can be completed. Drones also do not influence the environment as much as traditional airplanes do. Due to less

fuel consumption (or lack of it in a case of vehicles powered with the use of batteries), drones do not emit CO₂ into the atmosphere. What is more, there are some areas which are inaccessible for manned aerial vehicles such as mountainous regions or high-risk places. In these instances, UAV can be used to acquire necessary information without risking human life. Also for rotary wing UAV platforms, no runway is required, what can be useful in the necessity of performing vertical take-off or landing.

On the other hand, drones also have many limitations. Due to the small size of many drones, it is impossible to mount professional, multi spectral, high-resolution camera on board. Low-cost UAVs usually have amateur cameras which cannot capture high quality images. As a consequence, big overlaps between photos and strips are necessary to acquire good resolution of ground objects. Also, accurate IMU devices are replaced with the smaller and less sensitive ones. In cheap drones, the GNSS navigation system uses code-based positioning mode, which cannot ensure very accurate coordinates and direct georeferencing (Remondino, et al., 2011). Size and weight of the unmanned platform could be also a drawback due to weather conditions, as the platform is not very stable while wind gusts are present. However, low-cost drones are not the only ones available on the market. There are also professional drones, which are dedicated to surveying. Their cost is higher (sometimes even comparable to the manned vehicles) but they are bigger, have the possibility to mount better cameras, both IMU and GNSS system are more accurate.

Knowing advantages and also limitations of Unmanned Aerial Vehicles is the first step to examine how they can be used in photogrammetry.

2.1.5 Phantom 3 Advanced

The low-cost drone Phantom 3 Advanced is going to be employed to acquire images (Fig. 2). One may say that it is consumer-grade drone which is very popular among the community, commonly used for aerial photography and as entertainment. On the contrary, it fulfills most of the criteria necessary to adopt it as a mobile mapping system. Both IMU and GNSS navigation systems allow it to perform automated aerial survey with sufficient accuracy. Phantom 3 Advanced is a quadcopter with a built-in camera and three-axis gimbal which maximize stability in roll, pitch and yaw directions with minimizing both weight and size. It is produced by the DJI Company. Characteristics of the drone can be found in Phantom 3 Advanced User Manual (DJI, 2015). It's producers emphasize it's most valuable aspects: the 2.7K camera and its 94° field of view, vision positioning system,

GPS+GLONASS dual positioning system, 3-axis stabilization gimbal and smart flight battery with charging level indicator. The detailed specification is shown in Table 1. Analyzing drone capabilities, maximum speed and maximum flight time seemed to be the most relevant limitations. Approximately 20 minutes of flying time is not satisfactory while surveying large-scale areas. Also, the lack of a separately mounted camera is a drawback as each survey might require lens and resolution suitable for its purpose.

Table 1 Phantom 3 Advanced specifications, Source: (DJI, 2015)

Aircraft	
Weight (with battery)	1280 g
Max speed	16 m/s
Max flight altitude	6000 m
Max flight time	App. 23 min
Operating Temperature range	0°C to 40°C
Remote Controller	
Operating Frequency	2.400 GHz – 2.483 GHz
Video Output Port	USB
Intelligent flight battery	
Capacity	4480 mAh
Voltage	15.2V
Battery Type	LiPo 4S
Energy	68 Wh
Operating Temperature	-10°C to 40°C
Max charging power	100W
Camera	
Sensor	Sony EXMOR 1/2.3” Effective pixels: 12.4
Lens	FOV 94° 20mm f/2.8
ISO range	100-3200 (video) 100-1600 (photo)
Electronic Shutter speed	8s – 1/8000s
Image size	4000x3000
Photo	JPEG, DNG
Video	MP4/MOV
Supported SD cards	MicroSD

DJI also released DJI GO, which is a mobile application designed specifically for its products. It allows to manually control all the flight parameters including gimbal position, camera parameters, and flight modes. Unfortunately, mission planning module is not highly developed and restricts user possibilities to plan an autonomous flight that could accomplish photogrammetric requirements. Therefore Pix4D Capture application was adopted to design the flight plan.



Figure 2 Drone Phantom 3 Advanced

2.2 UAV Photogrammetry

As it was mentioned in a previous chapter UAV became an alternative to the classical photogrammetry. Replacing a traditional airplane with a pilot on board with an unmanned aerial vehicle brought many changes into the photogrammetry field. First of all, capturing photos changed significantly. Considering flight height, endurance, higher platform instability and type of onboard camera as its many benefits, however drawbacks could also be found in comparison to classical methods.

Some people believe that UAV photogrammetry is capable of filling the gap between classical photogrammetry and terrestrial close-range photogrammetry supported by laser scanners. However, there is also a significant group, who consider UAV platforms as the only supplementation of classical methods. Figure 3 illustrates the available geomatics techniques and where UAV photogrammetry finds its place, while Table 2 presents a comparison between close-range, aerial and UAV photogrammetry.

Table 2 Features of aerial, close range and UAV photogrammetry. Source: (Eisenbeib, 2009)

	Aerial	Close Range	UAV
Planning	automatic, semi-automatic	manual	automatic, semi-automatic, manual
Data acquisition/flight	assisted, manual	autonomous, assisted, manual	autonomous, assisted, manual
Size of the area	km ²	mm ² - m ²	m ² - km ²
Image resolution/GSD	cm - m	mm - dm	mm - m
Distance to the object	100 m – 10 km	cm – 300 m	m - km
Orientation	normal, (oblique)	normal, oblique	normal, oblique
Absolut accuracy of the initial orientation values	cm - dm	mm - m	cm -10 m
Image block size/number of scans	10-1000	1-500	1-1000
Special applications	large scale areas (mapping, forestry, glaciology, 3D city modelling)	small scale areas and objects (architectural and industrial photogrammetry)	small and large scale areas, also inaccessible areas and dangerous objects)

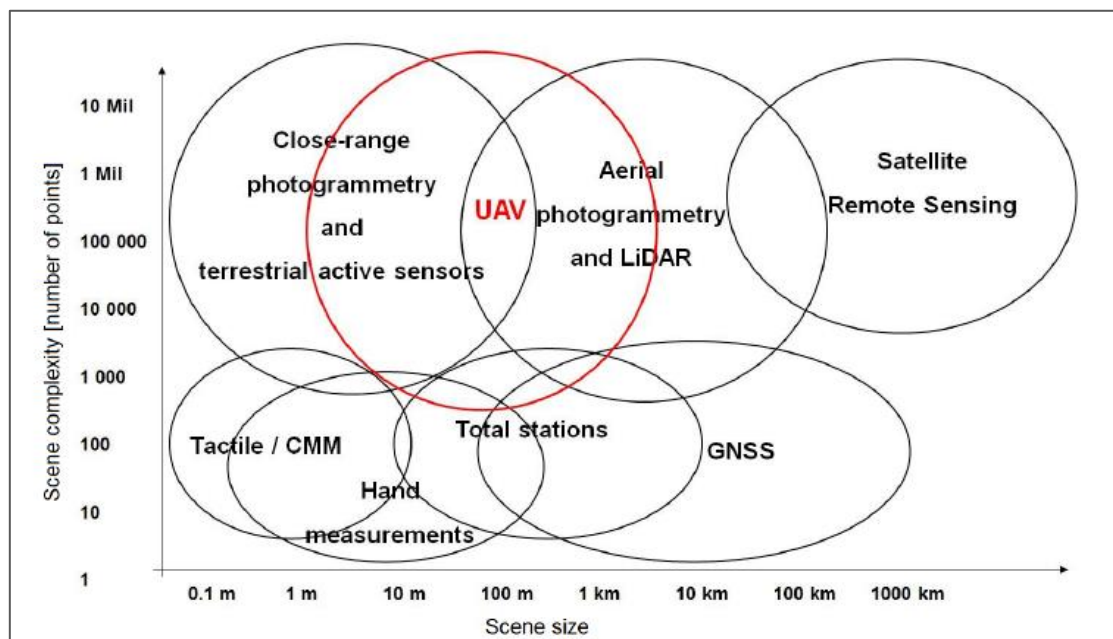


Figure 3 Various surveying techniques for 3D recording purposes Source: (Remondino, et al., 2011)

In addition to the table, it could be said that UAV flights seem to be cheaper, more accessible and easier to deploy than classical measurement methods. They are less dependent on weather and give the possibility to acquire vertical, oblique or targeted photos during one flight mission. However, due to lower flight altitude and smaller size of CCD matrices in the camera, a lot more photos are required to cover the same area as with the use of aerial imagery.

2.2.1 Flight plan

A properly designed flight plan is an essential part of any photogrammetric survey. The coordinates of each image should be precisely determined in order to achieve required ground sample size and overlaps between photos. A requirement of stereo photogrammetry is that every point on the ground is imaged in at least two metric photographs. With the 50% overlap between photos within a strip, the requirement is met. However, due to the fact that the earth is not an ideal flat surface, ideal imaging configuration doesn't exist and the plane always experiences some external influence, the 50% overlap is not sufficient. To ensure appropriate coverage between photos 60% and 25%-30% for forward and side overlap are used respectively. Nevertheless, in UAV photogrammetry even 80% overlaps are necessary to obtain accurate and dependable results. It is mainly due to low-cost cameras with worse resolution and instability of the drone. Another thing to consider while producing the flight plan is the required resolution on the ground, usually defined as Ground Sample Distance (GSD) size. GSD is a distance on the ground which represents one pixel on the image. The lower the GSD, the higher the photo spatial resolution and more visible details. As a consequence, the required accuracy of the photogrammetric end products determines flight height. The higher the flight level is, the bigger the GDS value becomes. One more thing to examine is the camera focal length. In classical photogrammetry, cameras with different objective lenses are used for various applications. Different fields of view and principal distances vary depending on the nature of the surveyed area. As it was mentioned earlier, many drones do not use professional cameras and the choice of a proper camera is not an important part of flight planning. However, knowing the distance of the camera constant is essential to compute the image scale (Eq. 1, 2).

$$M = W * cc \quad (1)$$

$$GSD = M * ps \quad (2)$$

Where M - image scale, W – flight height above ground, cc – camera constant, GSD – Ground Sample Distance, ps – pixel size of CCD camera.

The final product of flight planning is usually divided into two parts. One of them is the navigation plan which consists of a map with the places of where the photos should be taken. The map also presents areas of interests and obstacles in the flight plan. Another document is a sheet with specifications about camera parameters, flying height above ground, image scale, base, flying speed, length and width of the block, etc. (Kraus, 2007). Nowadays, the UAV photogrammetry final form of the flight plan is slightly different. Usually, available software (e.g. DJI GO, Litchi, Mission Planner) allows a user to enter essential parameters such as area extent, overlaps and flight height. Knowing drone specifications like the camera constant and image resolution, the software can compute the coordinates of the images, which determines the flight path. The list of coordinates is imported to a drone and a fully autonomous flight mission can be performed.

2.2.2 Post processing

Also, the software requires some modification in relation to classical photogrammetric programs such as SocetSet, Photomode or Leica Photogrammetry Suite. Due to many irregularities in flight such as tilted photos, fluctuations in scale, inaccurate exterior orientation parameters and deviations in photos overlaps, the classical software has difficulties in processing photos obtained from a drone. Also, the images distortion, radiometric variations and blurred photographs caused by wind gusts are obstacles in generating efficient photogrammetric products. All of these factors contribute to developing based on Computer Vision (CV) drones dedicated software. One of these programs advantages is a relatively short time of the fully automated process of image matching, possible due to big overlaps. No measurements in Gruber regions are required and feature – based algorithms are implemented to align photos. Implemented methodology has its origins in Structure from Motion (SfM) technique. The SfM method estimates three-dimensional structures from two-dimensional image sequences. It allows to calculate camera orientation parameters and adjust the whole block of images at the same time. To determine exterior orientation parameters the process of aerotriangulation needs to be done. Nowadays, bundle block adjustment method is adapted as the most complex method in photogrammetric

software. Relations between image coordinates and object coordinates are computed directly based on the collinearity equation. The image coordinates and the associated perspective center of a photograph define a spatial bundle of rays (Fig. 4). The elements of exterior orientation of all the bundles in a block are computed simultaneously for all photographs (Kraus, 2007).

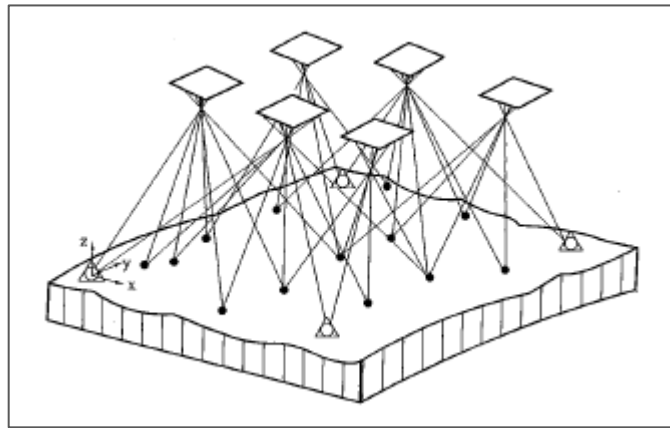


Figure 4 Principle of bundle block adjustment.
Source: (Kraus, 2007)

Examples of computer vision software such as Agisoft PhotoScan and Pix4D Mapper are described in more detail in following chapters of the thesis. With the photos obtained from a drone, the following outputs could be generated by software: 3D point clouds, triangulated mesh surfaces, orthophotomaps, Digital Surface and Elevation Models. Also, volume and surface measurements are possible to execute.

2.2.3 Ground Control Points

Ground Control Points (GCP) are points of known coordinates marked on the terrain. They are usually measured with traditional survey methods as their values should be established very precisely. They are used to georeference photos, which means to calculate the scale, orientation and absolute position of the products in a preferred coordinate system (Madawalagama, et al., 2016). Depending on the feature they could be natural such as the centers of sewer drains or artificial such as crosses or circles painted on the road. Depending on dimension they could be 3D, 2D or 1D. And finally, depending on the function, they can account in the adjustment or serve as check points to validate the accuracy of the final product. Ground Control Points should be located on a flat surface within the area of study,

especially in the corners of the block of images. The GNSS system mounted on the drone can also acquire the coordinates of the photos and georeference products in a space. Although as it was mentioned earlier (Section 2.1.4), due to low-cost and size of drones, the accuracy of these GNSS receivers is not satisfactory and GCPs are necessary to increase the accuracy and obtain reliable product placed at exact position on the Earth. With the use of CV software, only few GCP (but more than three) evenly distributed over the study area are enough to georeference block of images. Usually, a subset of Ground Control Points can be used as a Check Points (CP). These points with known coordinates serves as a validation of image processing. It means that they are not included into bundle block adjustment computations but the difference between their coordinates and interpolated surface determines the accuracy of adjustment.

2.3 Digital Elevation Model

Both the Digital Surface Model (DSM) and Digital Elevation Model are 2D maps, where every point has coded information about its altitude. The difference between them is that DSM presents both natural and built features on the earth surface, while DEM is the representation of bare-earth surface without any powerlines, buildings, bridges, trees and other types of vegetation. As the DSM represents the highest elevation of the terrain, earth surface is then modelled only over open areas without roofs of the buildings and tree canopies. A difference between these two models is illustrated in Figure 5.

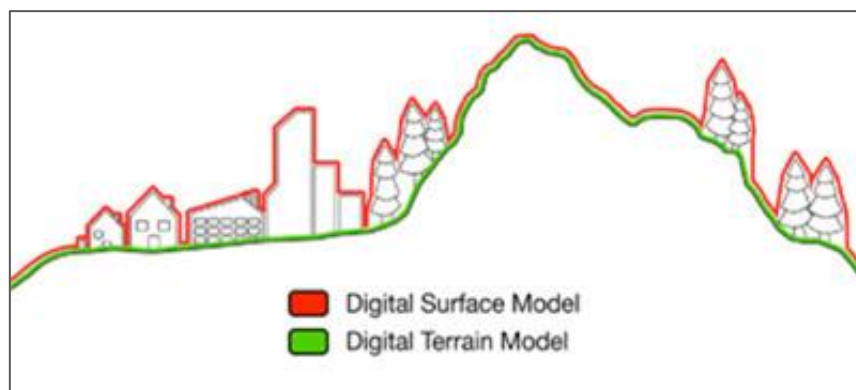


Figure 5 Difference between DSM and DTM/DEM
Source: geoimage.com.au

Moreover, there is also another term for numerical representation of the Earth surface - Digital Terrain Model (DTM). It is described as 3D representation of terrain surface consisting of X, Y and Z coordinates in digital form. As the DEM and DSM it stores algorithms to calculate height between points but in advance it includes other geographical elements such as ridges and breaklines. In general, DTM is vector data with evenly distributed points storing information about elevation (Fig. 6). The Digital Terrain Model could be interpolated into Digital Elevation Model and then augments DEM by including linear features of bare-earth surface. Nevertheless, in many resources and literature, DEM and DTM terms are used as synonyms without exposing any difference.

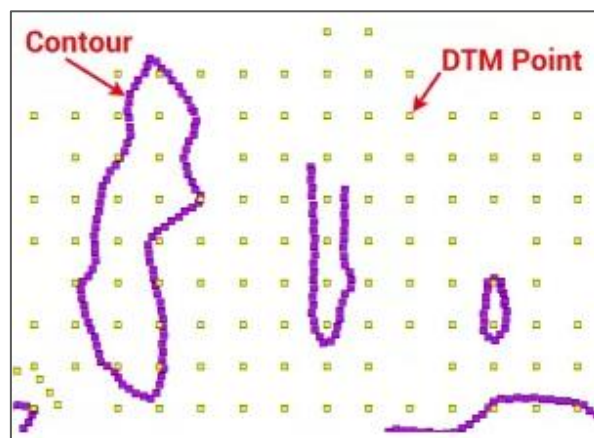
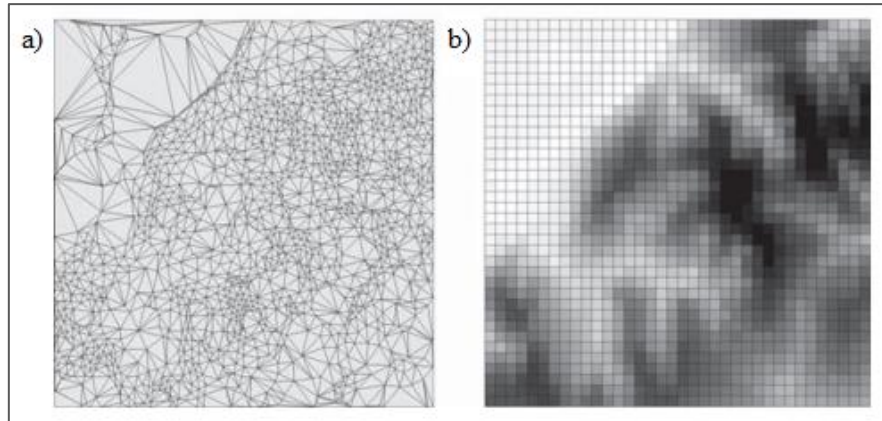


Figure 6 Digital Terrain Model
Source: gisgeogrpahy.com

Most commonly used DEM are regular grids, triangular irregular networks (TIN) and contour line models. These representations of terrain surface have specific strengths and weaknesses due to different assumptions. The main advantage of TIN is its possibility to present mountainous areas, high relief and rough surfaces very precisely (Fig. 7.a). Points storing elevation values are triangulated using Delaunay's criterion and form irregular network of triangles. Because of its irregularity, software algorithms are more demanding and time-consuming. In comparison, grid models due to simple structure are easy to be reconstructed and their basic unit is a cell (Fig. 7.b). However, their significant drawback is simplifying the complexity of earth's surface. Although TIN dataset is considered to be the most accurate representation, most of the standardized DEMs have been generated using grids as it is the simplest and the most effective approach in terms of storage and manipulation of data (Liu, 2008).



**Figure 7 On the left: TIN model, On the right: grid model.
Source: (Hengl & Evans, 2009)**

2.3.1 Applications

As the DSM provides essential knowledge about natural and built objects on earth it is commonly used in 3D modelling, view obstruction in urban planning, telecommunications and vegetation management. However, DEMs play a great role in terrain-related applications, as a source of information about elevation. They are considered to be significant geospatial datasets due to the versatile possibilities of their use. In geomatics they are used for orthorectification of aerial imagery, cartographic representations and three-dimensional visualizations of earth's surface. Its application is also found in environmental sectors contributing to hydrological modelling, coastal monitoring, terrain analyses, water management, forest inventory and climate impact studies. Other utilizations are road planning, flood risk analysis, land-cover, land-use classification and object detection (Polat & Uysal, 2015).

2.3.2 Acquisition

To acquire information about ground elevation, a number of possible solutions are available. Traditional surveying methods with the use of total station and GPS receiver provide accurate results but due to the duration of gathering data, process are considered ineffective and are not commonly adopted in great scale projects. Since DEMs are usually produced for extent areas of Earth, remote sensing technologies seem to be the most efficient way to gather data. Examples of these methods are aerial photogrammetry and satellite interferometry, but in recent years, due to increase in effectiveness of the process, LIDAR

data acquisition become a very powerful way to produce DEMs. Airborne Light Detection and Ranging is an active remote sensing technology, which uses light in the form of the pulsed laser to measure ranges to the Earth. The LiDAR output is a three-dimensional georeferenced point cloud with information about the shape of the Earth and objects on the ground. With active sensors, LiDAR data acquisition may be performed both during the day and night, and data is free of shadows. However, the main advantage of the LiDAR system is its capability of detecting multiple return signals for a single transmitted pulse. The possibility of penetrating through vegetation which results in obtaining ground points under trees overcomes the limitations of photogrammetry for DEM generation, especially in forested areas.

As the desired target for DEM generation is bare-earth points, the process of filtering data is essential. There are many different methods used to separate raw LiDAR data into ground and non-ground points. Some of them are Interpolation-based filter, slope-based filter, morphological filter, segmentation-based filter or K-mean clustering. Most of them use height difference as the measurement and base for computations (Liu, 2008).

Prior to recognizing the LiDAR method as the most effective of collecting three-dimensional information, the accessible software uses data filtering algorithms dedicated to the 3D point cloud which is characterized by multiple return signals. As a consequence, extracting non-ground points from a point cloud generated from drone aerial images, due to obtaining DEM in Agisoft PhotoScan and Pix4D might not be satisfactory. As an alternative solution, images classification can be proposed.

2.4 Image Classification

Remotely sensed data in the form of satellite and aerial photography with the aid of image classification analysis is a commonly known source of information about the land cover. A variety of different classification methods precisely described in the literature exist. Depending on the nature of data such as data distribution, a number of features and linear and nonlinear separability, the adequate practice can be determined.

Classification is the process of sorting pixels into a finite number of individual classes or categories of data, based on their values. It is executed on the basis of spectral or spectrally defined features, such as density, texture, etc. in the feature space (Bhatta, 2008). There are two different approaches to accomplish the classification process: supervised classification

and unsupervised classification. The main difference is way of assigning the pixels to classes. In the supervised method, the first step is to select pixels that represent patterns or land-cover features. These training samples are used by software to form class spectral signatures. Later, the rest of the image pixels are examined and assigned into respective class with similar characteristics. On the contrary, in unsupervised classification pixels are grouped based on the reflective properties of pixels. These groups of pixels are called clusters and their number is determined by the user before the process run. After classification, the user manually attaches a land cover class to the resulting spectral class. The unsupervised classification method is usually used when there is not enough knowledge about the data and determining training samples is problematic. Workflow for both approaches is presented in Figures 8 and 9 (ESRI Support, 2017).



Figure 8 Supervised classification scheme

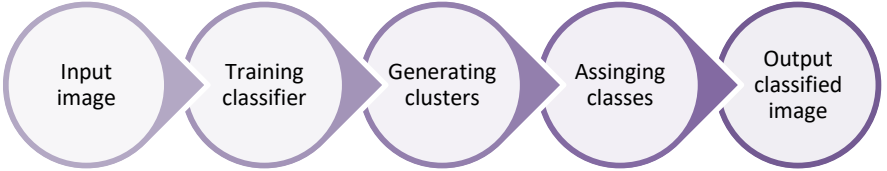


Figure 9 Unsupervised classification scheme

Another distinction within the classification process is a pixel-based and an object-based approach. Pixel-based traditional procedures analyze the spectral properties of every pixel without taking into account neighboring pixels. The main disadvantage of this method is that it may result in salt and pepper effect on a classified map. Object-based classifiers do not use only spectral signatures but also include spatial and contextual information related to the pixel of interest (Weih & Riggan, 2010). The first step is segmentations when an image is

dissected with respect to the object representing pixel groups obtained with criteria such as shape, compactness, scale factor, etc. Afterward, the segments are classified according to the classification algorithm (Akar, 2017). An important factor to consider while determining the classification approach is the spatial resolution of the input image. With medium and low spatial resolution both methods should provide comparable results. However, in the case of high spatial resolution, object-based approach outweighs the traditional one. Due to the fact that objects on the map are represented by several pixels, performing segmentation will result in more accurate and perspicuous map.

2.4.1 Image classification algorithms

A separate thesis could be written describing different algorithms used in the process of image classification and their analyses. A great number of different techniques and their modifications has been developed and implemented in many software packages. As the image classification process is going to be performed in ArcGIS Pro software, description of classification algorithms covers only these, which are available in the program: ISO Cluster, Maximum Likelihood, Random Trees and Support Vector Machines.

ISO Cluster classifier (ISO)

It is used to perform unsupervised classification. In the iterative process minimum Euclidean distance is computed to assign each candidate cell to the cluster. At the beginning, every cell is assigned to the closest mean, which was created arbitrarily. Next, based on distance attribute, new means are calculated for clusters and cells are assigned to the closest means again. And the process repeats until migration of cells from one cluster to another is minimal, so all the clusters become stable. Like in other unsupervised classification methods it is essential to establish a number of clusters before performing computations. Also, the number of iterations is very often determined by the user. ISO cluster algorithm implemented in ArcGIS has a capability to handle very large segmented images with extending attribute tables (ESRI Support, 2017).

Maximum Likelihood classifier (ML)

It is one of the oldest and most popular methods of supervised classification. In this traditional approach, the probability theory is applied to the classification task. With the assumption that the distribution of training samples is normal, each class is characterized by

means and variance-covariance matrix. It allows determining the probability that the given cell in the input raster belongs to the particular training set. Probability depends on the distance from the cell to the class center, but also on size and shape of the class in spectral space. All class probabilities are computed for each cell and the cell is assigned to the class with the highest probability value (Bhatta, 2008).

Random Trees Classifier (RT)

The definition provided by ESRI says that this classifier is a collection of individual decision trees where each tree is generated from different samples and subsets of training data. It indicates similarity to the commonly used in literature Random Forest classifier. It is supervised machine-learning method based on creating a number of classification trees used to determine a set of rules that establish an optimal classification tree to be used for final classification. To make final a decision each tree has a vote and decisions are made in rank order of importance. Random Forest partitions data into training and testing samples using stratified random selection, and the testing data set are used for performance validation. This technique is resistant to overfitting (Wendel, et al., 2015)

Support Vector Machines Classifier (SVM)

Using this supervised classifier, classes are separated based on statistical learning theory, with a decision surface which maximizes margin between them. Data points closest to the decision surface are called support vectors. In the case of linearly separable classes, two parallel planes maximizing the margin between classes are formed and an optimum hyperplane is placed in the middle. If it is not possible to separate classes linearly, vectors are transformed into higher dimensional feature space to optimally separate data into different classes. Originally, the SVM technique was used to separate two classes, however, with time, the multi-class approach was developed. As it is a binary approach, data objects are progressively distinguished among pairs of classes. The method is also less susceptible to noise and correlated bands (Yilmaz, et al., 2016).

2.4.2 Accuracy assessment

Knowledge about the accuracy of classified maps is the base to determine whether the generated product is reliable enough for further usage. Comparing the image visually with its classified result allows to detect errors in wrongly classified areas and estimate their size.

Nevertheless, it doesn't provide any numerical and absolute values, so the map has limited applicability. However, visual evaluation of classified map is not the only way to determine how accurately the process has been done. The most common quantitative method of characterizing image classification accuracy is known as confusion matrix. It provides a comparison between classification result and reference data. Reference data should be ground truth data, which should be based on a different information source. These could be GPS observations collected in the field, randomly distributed over the study area, but also manual image digitization of random set of points. The result of two datasets comparison is a confusion table with columns representing reference data and rows demonstrating classification results (Tab. 3). Diagonal elements indicate numbers of correctly identified pixels, while off-diagonals elements present misclassified pixels. Last row and last column are omission and commission errors respectively. Omission error also known as producer's accuracy indicates pixels, which were omitted by the classifier. It means that pixels were assigned to the wrong class, while they should be classified as something else. Commission error is known as user's accuracy meaning that classifier committed a label to those samples which actually belong to other labels. The overall accuracy of a classification map known as Kappa parameter is computed by dividing all correctly classified pixels (sum of the major diagonal) by the total number of reference pixels in error matrix (Eq. 3).

$$\omega = \frac{\sum_{i=1}^{nc} e_{ii}}{NT} * 100 \quad (3)$$

Where ω – overall accuracy in percentage, nc – total number of classes, e_{ii} – element in the i^{th} row and i^{th} column, NT – total number of pixels.

Generally speaking, image classification is time-consuming and complex process. Usually, to classify an image correctly, many steps need to be taken. They include image segmentation, training samples selection, training classifier and finally classifying with accuracy assessment. Most of them are iterative operations and require few attempts to find optimal parameters for the classified dataset. Considering the nature of input data, classification scheme and algorithms, expected results and acceptable accuracy, an accurate classified map could be generated. One of the objectives of this thesis is to examine different classifications methods and determine which of them is the most suitable for studied dataset.

Table 3 Confusion matrix

		Reference					
Classification	Class	1	2	3	i	Row total	Commission error
	1	$X_{1,1}$	$X_{1,2}$	$X_{1,3}$	$X_{1,i}$	Σ	$X_{1,1}/\Sigma$
	2	$X_{2,1}$	$X_{2,2}$	$X_{2,3}$	$X_{2,i}$	Σ	$X_{2,2}/\Sigma$
	3	$X_{3,1}$	$X_{3,2}$	$X_{3,3}$	$X_{3,i}$	Σ	$X_{3,3}/\Sigma$
	i	$X_{i,1}$	$X_{i,2}$	$X_{i,3}$	$X_{i,i}$	Σ	$X_{i,i}/\Sigma$
	Column total	Σ	Σ	Σ	Σ	NT	
	Omission error	$X_{1,1}/\Sigma$	$X_{2,2}/\Sigma$	$X_{3,3}/\Sigma$	$X_{i,i}/\Sigma$		ω

2.5 Software

With the advent of UAV photogrammetry, drone dedicated software has begun to be created and released. At least two of them became very popular and commonly used. Both of them are commercial programs with a price 3499\$ and 2600€ per year for Agisoft PhotoScan and Pix4D respectively. Both of them are introduced as advanced and complete mapping and modeling solutions to convert images into geo-referenced mosaics and 3D models. Both of them have similar step-by-step procedure to process data and acquire final products. While setting the project and loading photos, programs automatically read image metadata such as approximate coordinates of images centers, flight altitude and used camera parameters. The first step of processing is image alignment when common points on images are searched and photos are matched. What is more, an approximate position for each photo is found and as a result of self-calibration, parameters of interior orientation are refined. In a consequence, a sparse point cloud is generated and a set of camera positions is formed. The next step is producing dense point cloud with the use of a dense stereo matching algorithm. Depending on the computer RAM memory and the number of photos, the process may take from a couple of minutes to a number of hours. The point cloud may contain gaps and holes at those locations where the image matching has failed (Bhandari, et al., 2015). However, the output can be edited or classified before the next step which is building a mesh. Mesh represents the surface of the object that could be also edited, smoothed, etc. The last step depends on the individual

purpose of the project, whether the user wants to texture 3D model or generate orthomosaic and Digital Elevation Model.

2.5.1 Agisoft PhotoScan

As the theme of the thesis is extraction non-ground objects in order to obtain DEM, a deeper look into point cloud classification and DEM generation algorithms is required. Agisoft PhotoScan provides two types of classification. One of them is automatic division of all points into ground points and non-ground points. Another one is a manual selection of points to be placed in a certain class from the standard list known for LIDAR data. An automatic classification procedure consists of two steps. At the first step, the dense cloud is divided into cells of a certain size. In each cell, the lowest point is detected. Triangulation of these points gives the first approximation of the terrain model. At the second step, a new point is added to the ground class, providing that it satisfies two conditions: it lies within a certain distance from the terrain model and that the angle between terrain model and the line to connect this new point with a point from a ground class is less than a certain angle. The second step is repeated while there are still points to be checked. The maximum angle for nearly flat terrain is recommended to be about 15° and higher value for terrain with steep slopes. Maximum distance determines the assumption for the maximum variation of the ground elevation at a time. Cell size should be indicated with respect to the size of the largest area within the scene that does not contain any ground points. With the classified dense point, Digital Elevation Model can be generated. Software provides three different methods of interpolation: disabled interpolation mode, which reconstruct DEM only on the areas corresponding to dense point cloud, enabled interpolation mode, which calculate DEM for all areas of the scene that are visible on at least one image and extrapolated mode, where the program generates holeless model with some elevation data being extrapolated (Agisoft LCC, 2016).

2.5.2 Pix4D Mapper

Also, Pix4D mapper software enables to perform point cloud classification and DEM generation. Nevertheless, the process is not as complex as in Agisoft PhotoScan. This program's algorithm takes as input the merged Raster DSM (Digital Surface Model), computes a classification mask that represents the terrain/objects and automatically generates

the Raster DTM (Digital Terrain Model). The main drawback is that users can only see DTM as a result of the process, without a possibility to display classified point cloud and visually assess its correctness. In the previous version of the software, the point cloud classification option was present and extracting ground points could have been done with more user influence. Currently, it is removed but Pix4D technical support team ensures that the module is under development and it is going to be reintroduced in future versions (Pix4D, 2016).

2.5.3 ArcGIS Pro

Differently from Agisoft PhotoScan and Pix4D Mapper, ArcGIS Pro is not drone dedicated software but as one of the most powerful GIS packages, it was going to be adopted for image classification process. The software is developed by the ESRI company, which derives the whole package of GIS programs such as ArcMap, ArcCatalog, ArcScene, ArcGIS Online and many more. ArcGIS Pro provides tools used for 2D and 3D mapping, performing advanced geospatial analyses, creating and managing datasets, working with imagery, preparing complex visualizations and other GIS related applications. The functionality of the image processing module allows working with rasters in different formats and may be adopted for various purposes. As image classification might be lengthy workflow with many stages of processing, ArcGIS Pro supports two approaches. One of them is Classification Wizard Module, which leads the user through the whole process step by step providing required guidance. And for more advanced users, separate tools such as *segmentation*, *training samples manager*, *classify*, *merge classes*, *assign classes*, *accuracy assessment* and *reclassifier* are available to perform classification in a desirable way. To ensure the independence of the classification process, the second approach was adopted by the author.

3 PROJECT WORKFLOW

This chapter contains five subchapters which describe a practical approach to achieve the aims of the thesis. Section one characterizes the area of study, measurements of Ground Control Points and the map presenting test field is included. Sections two describes the process of image acquisition. It is divided into two parts - mission planning and flight. All flight parameters are presented and their choice is explained. The main objective of the third section is an examination of image processing performance in two different software packages. Detailed workflow of image matching, bundle block adjustment and generation of point clouds, DEM, DSM, and orthophotomaps in Agisoft PhotoScan and Pix4D Mapper is described. The subchapter ends with a presentation of results of point cloud classification. Section four is the essential part of the thesis that describes the process of image classification in ArcGIS Pro software. It contains four stages which are data preparation, classification process, accuracy assessment and post-classification processing. The section also includes considerations about training samples creation, a performance of different classification algorithms and errors in the confusion matrix. The fifth section is the last stage of the project workflow. It focuses on DEM generation. Point cloud classified in Agisoft PhotoScan and point cloud classified in a process of image classification are used to produce two Digital Elevation Models. The models are compared and conclusions are drawn.

3.1 Study area and ground control points

The study area was established near Dragvoll, which is one of the campuses of Norwegian University of Science and Technology. The campus is located in the city of Trondheim, Sør-Trøndelag region, Norway. The size of the total image collection area is approximately 300 x 150 m. The test field has variations in terrain relief and comprises some buildings, roads, parkings, and vegetation.

The test field contains twelve evenly distributed Ground Control Points, marked just before the flight with the use of orange paint as 10x10 cm squares, which made them distinguishable from the background. Measurements of the points were carried out with the use of Leica VIVA GNSS receiver as a Real Time Kinematics (RTK GNSS) observations.

Each GCP was measured two times, with 30 epoch duration time. In order to obtain reliable results, measurements were executed with a time interval during different satellite configuration. One before the flight and one after two hours. The coordinate system of the acquired GCP north and east coordinates was EUREF89-UTM 32N, which is officially used in this area of Norway. Heights of GCP were established in NN2000, which is a reference system of normal heights. All of them are within an accuracy of 2 cm. Table 4 illustrates coordinates and accuracies.

A subset of these points was going to be used as Check Points. A map demonstrating their distribution is presented in Figure 10.

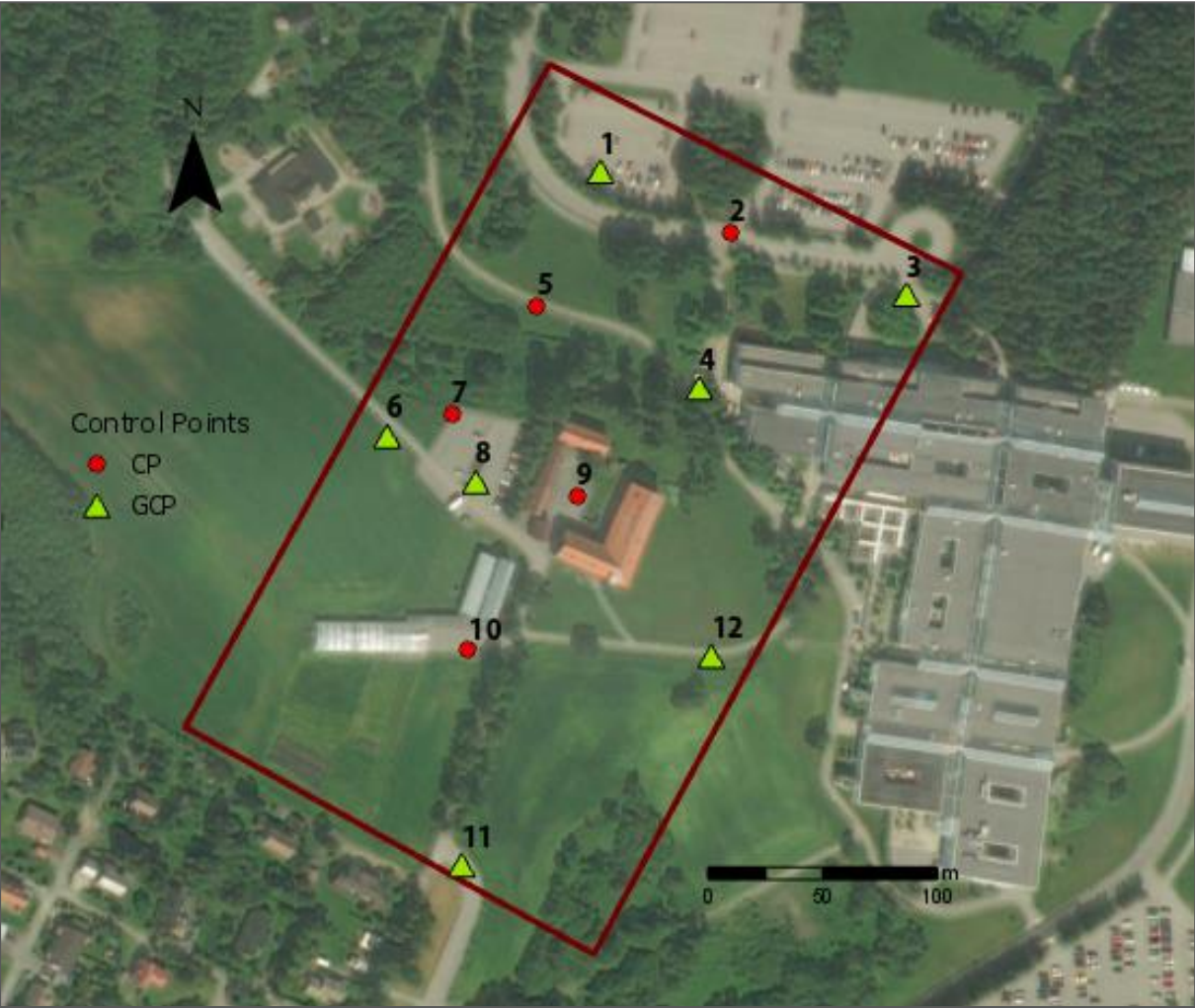


Figure 10 Study area with Ground Control Points (GCP) and Check Points (CP)

Table 4 Measured Ground Control Points

GCP	X [m]	Y [m]	Z [m]	Accuracy [m]
1	573229.523	7032076.641	163.028	0.008
2	573285.815	7032049.338	163.562	0.011
3	573362.918	7032023.120	163.506	0.011
4	573272.595	7031982.337	167.431	0.012
5	573202.033	7032017.627	170.070	0.011
6	573136.619	7031961.336	180.378	0.009
7	573164.818	7031970.109	180.625	0.009
8	573175.239	7031941.574	181.405	0.008
9	573219.200	7031934.813	181.964	0.010
10	573171.940	7031867.657	180.278	0.011
11	573169.049	7031774.917	179.871	0.008
12	573277.860	7031865.686	179.609	0.008

3.2 Image acquisition

3.2.1 Flight planning

In theory, there are many programs and applications dedicated to flight mission planning. In reality, most of the free-available applications but also some of the commercial software are not sufficient in terms of preparing fully autonomous, appropriate photogrammetric flights. Just before flight mission, Pix4D team released a new version of Pix4D Capture software. In the previous version, it was not possible to define two different overlaps – side and front needed to be the same which limited its applications. Nevertheless, the newest update was adopted to plan flight mission (Fig. 11). Phantom 3 Advanced camera characteristics such as camera constant and image pixel size were automatically loaded to the application after connecting drone with a remote controller. The study area was marked by indicating vertices on the map. Next, flight height, side and front overlaps were determined. In order to establish desired flight height, factors such as low regulations, maximum flight

time and ground pixel size were taken into consideration. Eighty meters above the ground decided to be an optimal value and compromise between all mentioned aspects. It doesn't exceed maximum acceptable flight height in Norway which is 120 m, the mission can be performed with the use of one battery, which gives approximately 20 minutes of flight time and GSD smaller than 5 cm can be obtained from this level. To ensure maximum stereoscopy and to avoid holes, overlaps of 80% and 70% were used for front and side overlap respectively. It resulted in 16 photos in each of the 5 strips required to cover the whole area of study.

Another important factor to determine was picture trigger mode. Images could have been captured in a motion or within 'stop-and-go' procedure when a drone would pause on each waypoint. With the author's previous experience, 'stop-and-go' procedure resulted in better accuracies while performing bundle block adjustment, as the camera mounted on Phantom 3 Advanced is not capable of acquiring high-quality pictures in a motion. Consequently, safe trigger mode was chosen. Drone speed was determined to be normal, as there was no need to fly slow or fast between corresponding waypoints. One more consideration was the place where to start a mission. As the flight height above the ground depends on the height of the start point, it was decided to be on the possibly highest point within the study area. So the minimum flight height above the ground was 80 m and greater in some areas of the test field. It ensured the minimum stereoscopy with 80% front and 70% side overlaps. Choosing the start point in lower areas would cause lack of sufficient overlaps and holes could appear while image matching.

To avoid hurry and confusions, the mission was carefully planned in the office before fieldwork. However, the list of coordinates which determined flight path and locations where the photos should be taken was uploaded to the drone in the field after connecting it to the remote controller.

The screenshot displays the Pix4D Capture mission planning interface. The top section shows a 3D aerial view of a mission area with a grid and flight path. The bottom section shows a settings panel with various mission parameters.

Top Panel (3D View):

- Altitude scale: 90, 80, 70, m
- Grid dimensions: 166 x 294 m
- Estimated flight time: 12 min : 55 s
- Buttons: RESET, START
- Battery indicator: 0%

Settings Panel:

- Angle of the camera: 90° (Slider from 0° to 90°)
- Front overlap: 80% (Slider from 0% to 90%)
- Side overlap: 70% (Slider from 0% to 90%)
- Look at grid's center: No (Buttons: No, Yes)
- Picture trigger mode: Safe mode (Buttons: Safe mode, Fast mode)
- Drone speed: Normal+ (Slider from Slow to Fast)
- White balance: Auto (Buttons: Auto, Sunny, Cloudy)
- Ignore homepoint: In takeoff checklist (Buttons: No, Yes)

Figure 11 Mission planning in Pix4D Capture

3.2.2 Flight

As in all types of field surveys, the weather is a crucial factor, which may affect final results. In UAV photogrammetry, the leading concern is the wind, which due to low weight of the drone can significantly change planned flight lines position. Also, the presence of sun can cause problems as it leads to the appearance of shadows on images. To avoid undesirable effects, the flight was performed during a cloudy and windless day. What is more, the mission was planned to be conducted late in the evening due to low crowds, which resulted in reducing the number of people and cars on the images. After uploading the earlier prepared mission, manual mode was changed to the automated flying mode. The aircraft raised to the height of 80 meters and moved towards the location of the first image. The drone was flying at the speed of 5 m/s and the whole mission lasted about 16 minutes. Eighty photos were taken with the across base of approximately 42 m and along the base of 20 m. All of the flight parameters resulted in 3,4 cm as the size of the ground pixel. During the entire time, the drone remained in the light of sight in order to change flight mode to the manual in case of any unexpected situations.

Some of the drones during the flight can record approximate values for all the exterior orientation parameters for each image. Timestamp, GPS location, elevation, roll, pitch, and heading are registered every time the camera's shutter is activated. Despite the presence of IMU on the drone board, Phantom 3 Advance is not capable of obtaining exterior orientation parameters. However approximate GPS location expressed in geographic coordinate system WGS84 and elevation are recorded and saved in the image EXIF files. The spectral resolution of acquired images is elementary, as the drone camera can record only three bands (red, green blue). Another output generated by the computer on a board is a log file which stores information about drone position during the whole flight.

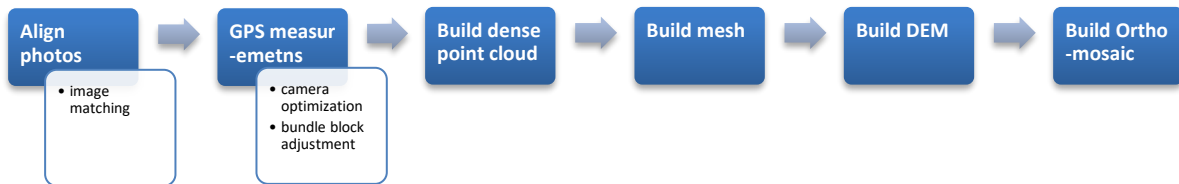
3.3 Image processing

Once the image acquisition was completed, photos were processed using different commercial 3D modeling software packages: Agisoft PhotoScan and Pix4D Mapper. The decision to use two programs instead of one was due to the possibility of comparison of obtained outputs and adopting more accurate orthophotomap for further analysis. The general workflow for both of them was similar and consists few fundamental steps such as photos

alignment, generating a dense point cloud, mesh, and Digital Surface Model and finally producing orthophotomap). Extracting non-ground points from dense point cloud in order to obtain Digital Elevation Model was a separate process, executed at the end of work in the program.

While processing data for the first time, the results were not satisfactory in both software packages. Errors on referencing points were about 10 cm for GCP and more than 20 cm for CP. With author's previous experience some steps were undertaken to find a reason for such a big inaccuracy. First of all, files with ground control points were examined to check if they didn't contain any mistakes. Next, in both programs, manual measurements of GCP were displayed and analyzed but even after correction of some markers which might have slightly better position, error values didn't change. Also, the coordinate's systems settings for GCP and photos were checked, but everything was fine. After many attempts and testing different workflow options, the reason was found. During the flight, for the first time, Pix4D Capture application was used by the author. Due to reducing flight time, the option to take photos in a motion without 'stop and go' procedure was chosen. It caused the problem for software as the camera mounted on Phantom 3 Advanced is a rolling shutter camera. It means that the camera records each image frame line by line from top to the bottom (it is opposite to the global shutter camera which records the entire image frame at the same moment). As the aircraft was moving during taking the photo, the camera and object relation was changed. It resulted in pixel displacement and caused problems for future matching and inaccurate camera parameters. However, Pix4D software has implemented a function to correct displacements and obtain better accuracy. As it is written on Pix4D website, most of DJI products take advantage of using this function. An attempt to process new project with this function enabled was made and quality report brought very positive results. GCP error values downturned into a couple of millimeters, and CP error values into a couple of centimeters which is very satisfactory while using the consumer-grade drone. Also in the recent version of Agisoft PhotoScan, rolling shutter camera option is available. Nevertheless, after processing data once again, improvements of the results were not sufficient to use it for further analyses. After investigating many web forums and Agisoft support website, the conclusion was that for DJI Phantom models 'stop and go' procedure is recommended. To provide a comparison between programs, another mission was planned (characterized in chapter 3.2.1) and workflow described below is related to images acquired for the second time.

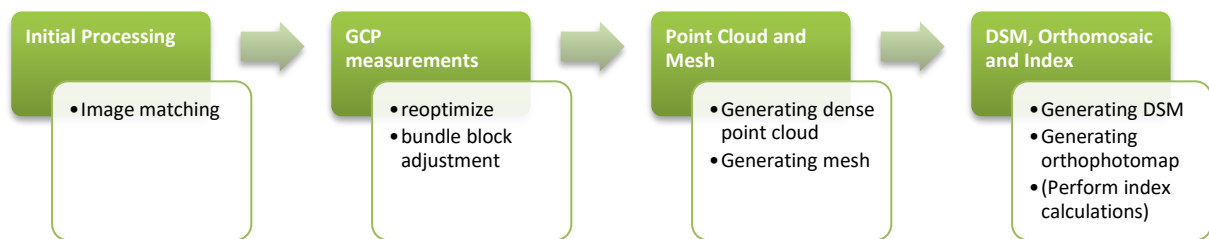
3.3.1 Agisoft PhotoScan



As the new project was created, settings were configured and photos with their metadata were imported into the program. Image quality function was run in order to check if any photos had been blurred or distorted in a way that could affect results. Gladly, all of the photos were accepted and a photo alignment process was launched. While defining parameters, the accuracy was set to be high and pair preselection method was set to be *generic*. As the coordinates of images were very inaccurate due to imprecise GPS receiver on a drone, the *generic* method seemed to be a better option than the *reference* method, which is more appropriate when camera positions are known. An output was computed camera positions with exterior orientation and camera calibration parameters, and sparse point cloud located in WGS84 coordinate system. As the next step was georeferencing with the use of GCP, the point cloud had to be transformed into GCP EUREF89 - UTM 32N coordinate system. Next, txt file, which stored information about GCP coordinates was imported to the software. The accuracy of GCP was set to be 2 cm, as it is the estimated accuracy of RTK GNSS measurements. Ground control points were measured manually and 5 of them were chosen to be check points (Fig. 12). The whole block of images was then adjusted using bundle block adjustment technique and errors on GCP and CP were computed. As the results were satisfying the point cloud could be done. The dense point cloud generation algorithm was then launched. Also, the filtering algorithms were used in order to exclude some outliers caused by noisy or badly focused photos. As the study area contains some small details but not really spatially distinguished, *Moderate* depth filtering mode was chosen as a compromise between *Mild* and *Aggressive* modes. The process took about 2 hours due to setting high quality as a desired final product. Based on the dense point cloud, mesh and DSM were obtained. For both of them, dense point cloud was chosen to be the source data. While generating mesh, the surface type was set to be *Arbitrary* as the option is recommended for

areas comprising buildings and not only planar surfaces. Also *enabled* interpolation mode was used to interpolate some surface areas within a circle of a certain radius around every dense cloud point. In the case of creating DSM, *enabled* interpolation mode is also the best option. It calculates DSM for all areas of the scene that are visible on at least one image. As there were a lot of buildings within the study area, the mesh surface type was chosen to generate orthophoto. In reference to the Agisoft manual this method is recommended for less common, yet quite demanded applications such as orthomosaic generation for facades of the buildings. No color correction was needed and blending mode was set as default, which means the option *mosaic*. Quality report of the process can be found in appendix nr 1.

3.3.2 Pix4D Mapper



Pix4D mapping software is described as specifically drone designed. Similar as in Agisoft, the first step was to import photos to the project and configure settings. Then, initial processing was done. As a result of key point extraction and image matching, sparse point cloud was generated. Also, the camera calibration parameters were computed in the process. To accurately georeference point cloud, ground control points were imported into the project. Manual measurements of GCPs were performed and to provide a comparison with Agisoft, the same 5 points were chosen to be control points (Fig. 12). Output coordinate system was set to be ETRS89 UTM Zone 32N. The bundle block adjustment method was used to adjust the whole block of photos and errors on GCP and CP were examined. Further, dense point cloud with mesh were generated. Significant parameters influencing the quality of 3D point cloud in Pix4D software are *Image Scale*, *Point Density* and *Minimum Number of Matches*. To obtain satisfying results, two first factors were set to be high and the point was decided to be correctly re-projected in at least three images. Dense point cloud describes object's surface, but it needs to be interpolated to form a triangulated irregular network in order to create mesh. The distance between mesh and the points of the point cloud is optimized by software to be

minimal, but this means that points of the mesh do not necessarily correspond to points of the point cloud (Pix4D, 2016). What was possible to determine before creating mesh was its *resolution*. As mesh surface was not going to be used as a crucial output in this thesis, default medium resolution was chosen. In the next step, Digital Surface Model and Orthomosaic were generated. Similarly, there were some parameters to determine, which affect the quality of output products. The minimum value for resolution of orthomosaic is established automatically based on results from initial processing. There is no limit for maximum value but since the orthophotomap is a key product of the next step, a possibly small value was chosen. Another option to consider are DSM filters. Using *Noise Filtering Function*, the altitude of erroneously generated points is corrected with the median altitude of the neighboring points. *Surface Smoothing* algorithm corrects areas with erroneous small bumps on the surface by flattening them. Three possible smoothing types are available: *Sharp*, *Smooth*, and *Medium*. The first one tries to keep sharp features such as corners and edges of buildings, while the second one assumes that sharp features exist because of noise and tries to smooth them. The last option is a compromise between them. Since some buildings are present over the study area and it is essential to have them presented distinctly, the sharp algorithm was deployed. As a method for raster DSM generation *Inverse Distance Weighting*, which uses weighting algorithm to interpolate surface between points. It is recommended for areas comprising building, while *Triangulation* algorithm based on Delauney triangulation is recommended for flat areas and stockpiles.



Figure 12 Manual measurements of control points in Agisoft (on the left) and in Pix4D (on the right)

After each of three described steps: *Initial Processing, Point Cloud and Mesh, DSM and Orthomosaic* software automatically generated reports with statistics and quality parameters (Appendix 2). It allowed the author to control the whole process and interpret results in reference to data nature and project purpose.

3.3.3 Accuracy Assessment

In this step, comparison among results from Agisoft and Pix4D was evaluated. As both of the software packages are considered to be Computer Vision software, they follow similar workflow but with the use of different algorithms. Therefore, for the further work, it is essential to compare the capabilities of different systems and evaluate which of them is more suitable for the survey purpose. Parameters crucial for analysis are presented in the table 5. Reprojection error characterizes the accuracy of image matching process. Each tie point is marked on at least two images which allow computing 3D position of the point using camera's internal and external parameters. Later, a 3D point is re-projected to all images where it appears. The distance between marked and reprojected point is reprojection error. In following rows, Root Mean Square Errors for Ground Control Points and Check Points on the ground and on the image are presented respectively. The formula for the given direction is defined as:

$$RMS = \sqrt{\frac{\sum ei^2}{N}} \quad (4)$$

Where ei is error for each point and N is the number of points. The seventh column depicts the ground sample distance, so the distance on the ground which represents one image pixel on orthophotomap. DEM resolution is possibly the smallest size of GSD proposed by software while generating DEM.

Analyzing Table 5 it can be stated that results obtained in Pix4D Mapper and Agisoft PhotoScan are comparable and have a similar level of accuracy. RMS errors for ground control points could serve as indicators of the whole project accuracy. Values smaller than 4 cm acquired during bundle block adjustment in both software packages are satisfactory in the context of using consumer-grade drone and measuring GCP in RTK GNSS mode. Respectively small values of RMS errors on control points indicates good quality of image

alignment process and block adjustment. Root Mean Square error on images expressed in pixels determines the accuracy of manual points measurements. Firstly, the results from Pix4D and Agisoft are difficult to compare among each other as the process was done separately in two programs and the difference in values doesn't depend on software but on user's measurements. On the other hand, with the author's experience, it may be assumed that measurements were carried out in the same way. Results obtained in Agisoft are very satisfying both for GCP and CP, as they fulfill criteria that projection error, which describes the Y-parallax between photos, should be smaller than 0.5 pix. In spite of a few attempts to reduce the image RMS error in Pix4D, it wasn't possible to fulfill the requirement after manual improvements of marker position. As the measurements were correct, another reason must have been found. The algorithm implemented in Pix4D calculates the weights for GCP based on zoom level in which they are measured on images. Points marked on a high zoom level are taken into account in bundle block adjustment more than points marked on a low zoom level. As control points are usually displayed in a different way on each image, different zoom levels were required to accomplish accurate measurements. It probably affected the overall accuracy and resulted in high projection errors. However, the reprojection error which indicates the quality of images alignment is more than four times better in Pix4D. Considering Ground Sample Distance for orthophotomap, Pix4D does slightly better than Agisoft. Nevertheless, Ground Sample Distance for Digital Elevation Model is almost three times worse than in Agisoft. The high value of DEM GSD in Pix4D software is due to the fact, that DEM is derived output created based on orthophotomap.

Table 5 Processing results from Pix4D Mapper and Agisoft PhotoScan

	Reprojec tion error [pix]	GCP RMS [cm]	GCP RMS [pix]	CP RMS [cm]	CP RMS [pix]	GSD [cm]	DEM resolution [cm]
Pix4D Mapper	0,173	3,70	0,840	6,12	0,770	3,36	16,85
Agisoft PhotoScan	0,769	3,57	0,393	7,91	0,366	3,44	6,88

As the results from two software packages are similar it was difficult to determine which orthophotomap should be taken for further analysis (Fig. 13). The visual examination also didn't bring any conclusions as despite few small details the products were almost

identical. Yet the orthophoto resolution is slightly better in Pix4D Mapper and GeoTIFF output file has three times smaller size, it was employed in chapter 4.4.

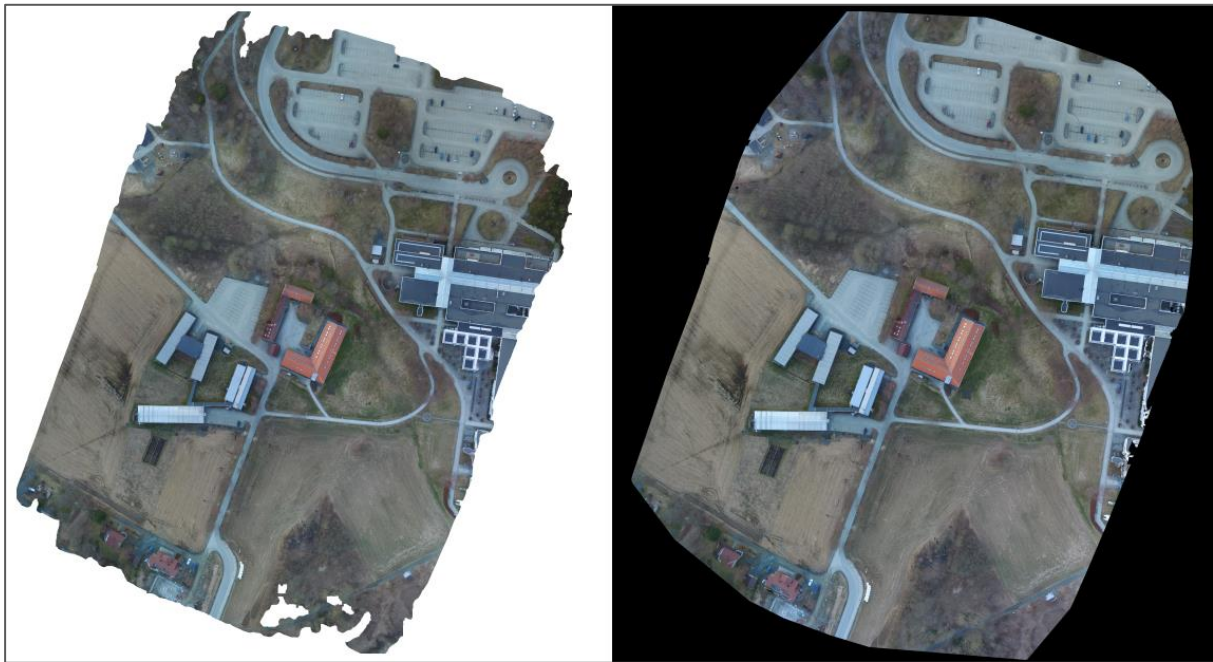


Figure 13 Orthophotomap generated in Agisoft (on the left) and in Pix4D (on the right)

3.3.4 Point cloud classification

The last step of workflow in Agisoft PhotoScan and Pix4D Mapper was classifying point cloud in order to generate Digital Elevation Model. Manual classification of dense point cloud was not a subject of this thesis so only automatic extraction of ground and low points has been performed.

In Agisoft software, the module *Classify Ground Points* was adopted. As parameters which control the process, the *maximum angle* which comprise the angle of slopes was set to be 20 deg, maximum distance which limits the distance between point and terrain was set to be 1 m and *cell size* which corresponds to the size of the largest area above the ground was set to be 80 m. In spite of the fact that these parameters correspond to the dataset in the best way, the results were not satisfactory. As it was suggested at the beginning of the thesis, algorithms implemented in Agisoft software are more suitable for point cloud acquired by LiDAR data than point cloud generated from images yielding in many holes and imperfections. Classification defects are presented in Figure 14. Upper pictures present classified point cloud and visible mistakes are marked with yellow ellipses, while pictures on the bottom illustrate

original point cloud. As it can be seen dense point cloud is not reconstructed correctly in some areas, especially close to the buildings and groups of trees. The observable problem is that the lowest parts of the objects are usually classified as ground points which is a mistake and leads to the generation of unreliable elevation models. However, to provide a comparison among different approaches, DEM based on classified bare earth points was generated.

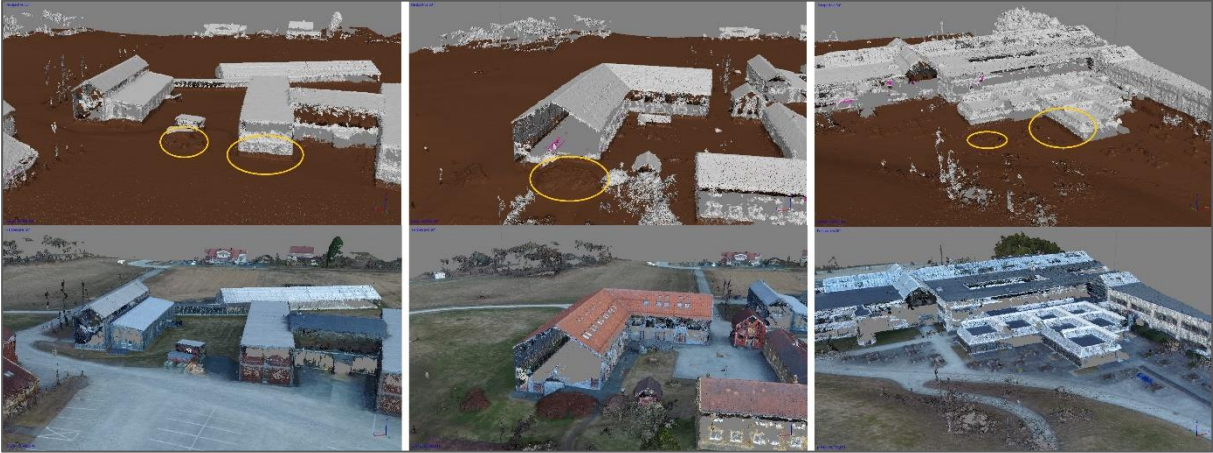


Figure 14 Blunders in classified point cloud

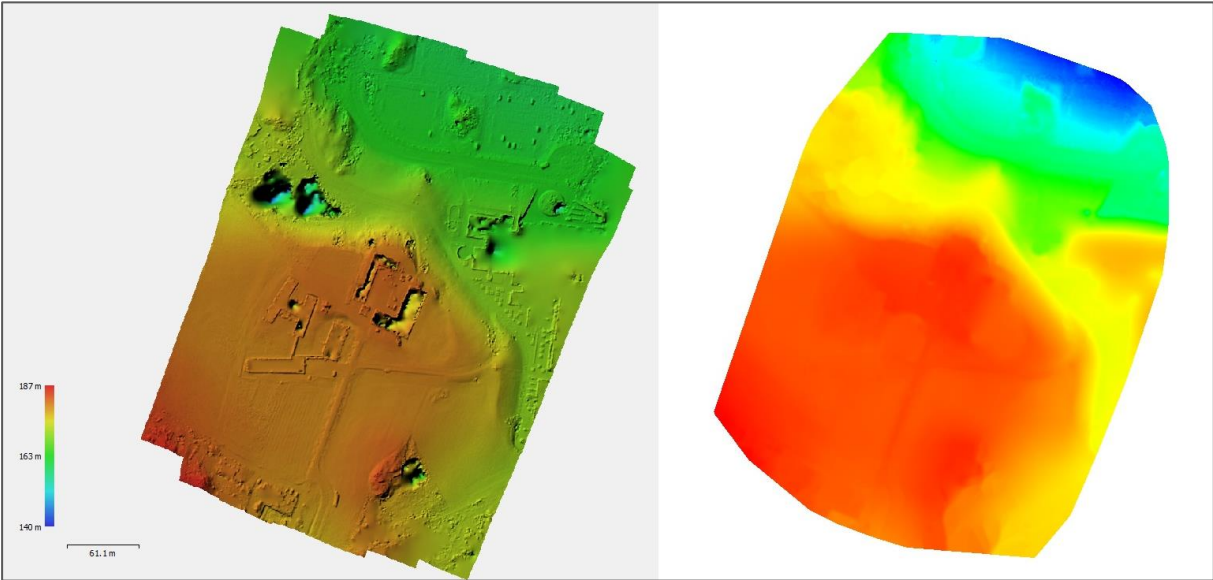


Figure 15 Digital Elevation Model generated in Agisoft (on the left) and in Pix4D (on the right)

Lack of possibility to examine classified point cloud in Pix4D did not allow to compare point clouds from two software packages. The only possible comparison was carried out based on visual interpretation of rasters representing Digital Elevation Models (Fig 15). As the resolution of DEM from Pix4D (16.85 cm) was almost three times bigger than DEM from Agisoft (6.88 cm), the model seems to be more smoothed and natural. DEM from Agisoft consists of more details, however, some outliers are noticeable in the areas close to the buildings. As there is no legend in the report from Pix4D it is not possible to point out differences in heights, though the colors distribution on two models is quite analogous.

As none of these models seemed to be satisfying, the author undertakes another approach which may lead to obtaining more reliable Digital Elevation Model. An idea based on image classification is described in the following subsection

3.4 Image classification

A great number of thematic mapping from remote sensed data is typically based on an image classification. Different variations of the method are commonly used by researchers and are described in detail in accessible literature. As a properly conducted classification process may bring very pleasant results, the author considers it as an alternative solution to prepare classified point cloud acquired from the drone's images for DEM generation.

To clearly present this problem, the chapter was divided into three parts: data preparation, classification process, and accuracy assessment. However, as image classification is a complex process, which requires many iterations and testing different parameters it was difficult to describe the whole procedure in a very structured way.

3.4.1 Data preparation

Orthophotomap exported from Pix4D Mapper in GeoTiff format was imported into a new project in ArcGIS Pro. Project workspace was set to be displayed in ETRS 1989 UTM 32N projected coordinate system. As ArcGIS Pro makes it possible to automatically upload the layer with World Imagery, the verification of raster placement could have been done visually. The orthophotomap raster was clipped with the mask polygon due to removing black background containing no data values and also areas close to the test field boundary as they may have contained some distortions (Fig. 16).



Figure 16 Original orthophotomap (on the left) and clipped orthophotomap (on the right)

Next, the image was segmented. Due to the fact that object-based classification is regarded as the best technique while working with high-resolution imagery, this approach was decided to be implemented. Thus grouping pixels into segments was an essential step before training classifiers. There were three parameters influencing the process of segmentation possible to specify in ArcGIS Pro software: *spectral detail*, *spatial detail* and *minimum segment size* in pixels. A range for the first two is between 1 and 20. *Spectral detail* value considers spectral differences of features on the raster. To obtain a smooth output, smaller values are recommended. On the contrary, high values allow classifying separate object even if their spectral characteristics are similar to other areas. *Spatial detail* value determines the level of importance given to the proximity between features. If objects are small and clustered, higher values are more appropriate. Smaller values lead to impervious and smooth surfaces. *Segment size* is expressed in pixels and ranges between 1 and 9999. Many attempts were performed to find the best parameters for examined raster dataset. Considering *spectral detail*, the only reasonable choice was value 20. All smaller values brought inadequate results, as the pixels were formed in large segments and single features weren't visible. A sensible value for *spatial detail* was around 14, as the rest of the values also led to generating too large segments. *Segment size* was set as default to be 20 pixels. Parts of the segmented image are illustrated in Figure 17.



Figure 17 Segmentation process: segmented image (above), original image (below)

3.4.2 Classification process

In order to perform supervised classification, training samples were required as an input data in the process. Groups of pixels with similar characteristics were created manually by indicating on the map polygons appropriate for each class. As it is reported in ArcGIS documentation, the recommended size of training samples should be at least $10*n$ pixels and maximum $100*n$ pixels for each class, where n is a number of spectral bands. Since the minimum limit needs to be accomplished in order to provide adequate information for classifying algorithm, the upper limit only suggests how many pixels are enough to obtain satisfying classification results. Thus, if specific objects on the image contain various pixel values it's better to create bigger training samples that provide complete information about objects. In the case of the categories were covering areas with similar extent, it would be beneficial to prepare samples containing an equal amount of pixels. Nevertheless, this rule can't be adopted to analysed orthophotomap, as classes vary significantly in a size and distribution.

Firstly, after analysing features present within the study area, eight classes were established: Roads, Grass, Ground, Green trees, No-leaf Trees, Bushes, Grey buildings, Red buildings. Ground was divided into Ground and Grass categories due to the fact that the images were captured in early spring, so not all vegetation was already green and spectral characteristics differ too much to put them into one class. However, after implementing classification, the results were not satisfactory (Fig. 18).

Table 6 Statistics of original training samples

	Statistics	R	G	B		Statistics	R	G	B
Grass	Minimum	25	41	23	Bushes	Minimum	32	32	32
	Maximum	121	130	111		Maximum	78	59	59
	Mean	57.78	71.05	54.95		Mean	60.96	43.92	45.28
	Std.dev	11.16	9.60	9.57		Std.dev	6.57	4.14	4.13
Ground	Minimum	24	28	34	Roads	Minimum	41	54	64
	Maximum	183	185	179		Maximum	213	223	245
	Mean	122.47	122.85	116.79		Mean	132	158.50	175.27
	Std.dev	13.13	12.89	13.18		Std.dev	17.03	19.47	22.11
Green Trees	Minimum	34	45	23	Grey buildings	Minimum	17	39	57
	Maximum	104	111	101		Maximum	151	190	223
	Mean	55.44	66.89	49.01		Mean	61.94	84.69	113.90
	Std.dev	8.40	7.67	8.16		Std.dev	9.45	12.15	13.89
No leaf Trees	Minimum	20	27	37	Red buildings	Minimum	61	42	47
	Maximum	187	187	190		Maximum	213	174	174
	Mean	80.93	82.64	84.32		Mean	142.80	101.50	102.56
	Std.dev	15.74	13.65	12.51		Std.dev	32.66	24.64	18.21

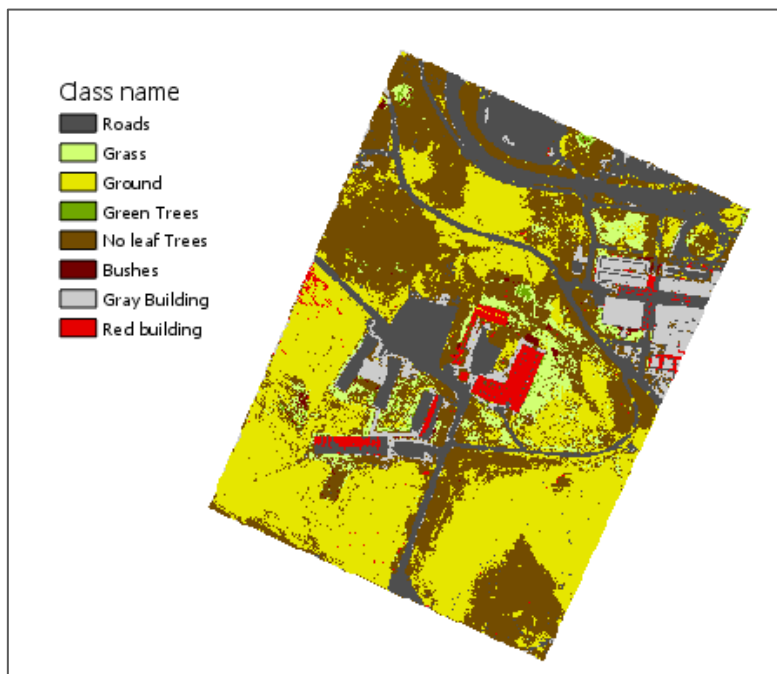


Figure 18 Results of pre – classification

In many parts of the map, the Road was misclassified with Grey Buildings and Grass was misclassified with Green Trees. Some parts of No-leaf Tress category appeared on

ground with unusual structure and resulted in noise with many small isolated regions of pixels. Evaluation of training samples was performed in order to find incorrectly created sites and make improvements (Tab. 6). As it can be seen in a table, there was a very high correlation between Grass and Green Trees classes. Their mean value is very similar in all three spectral bands. What is more, most of the classes have a very wide range of values and some of them are overlapping, which makes it very difficult for an algorithm to classify pixels into the exact class. As many pixels could belong to two or three different classes, the classifier needed to guess which class was more appropriate.

With all the conclusions, new training samples set was created. Green Trees category was removed as it led to too many confusions with pixels representing grass. Due to glass covering some roofs, one class representing these characteristics of pixels was created. As ground objects and forested areas were very problematic parts, an idea to separate them into subclasses inside main classes was implemented. Narrower classes would help the computer distinguish them from other categories during the classifier training process and they could be merged together in post-classification. New samples contain: Roads (1), Grass (2), Ground (3), No leaf Trees (5), Bushes (6), Grey buildings (7), Red buildings (8), Glass roofs (9), Crop (10), Forest (11) and High grass (12). Eleven training sites were created in a way to provide proportional samples distribution. More extensive classes such as Ground or Forest received a greater number of pixels (expressed in percentage) than small categories such as Bushes or Red buildings (Fig. 19).

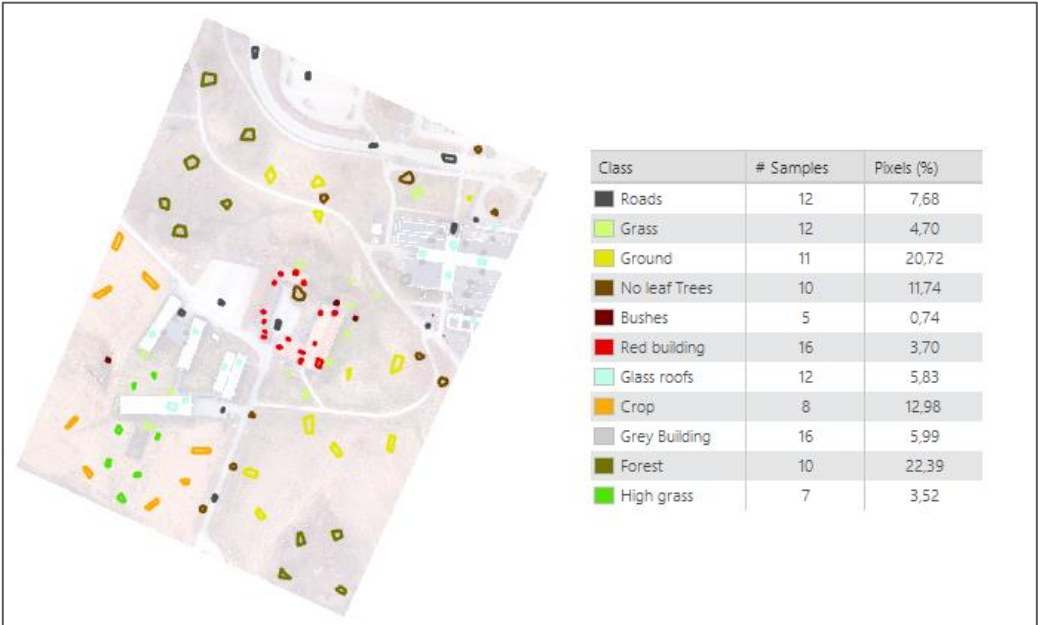


Figure 19 Training samples

Dataset was evaluated in order to check the correlation between classes. Regarding Table 7, there was still a strong correlation between Ground, Grass, Crop, High Grass and No Leaf Trees classes. Nevertheless, class's ranges were smaller and differences among other land cover categories were distinguishable.

Table 7 Statistics of training samples

	Statistics	R	G	B		Statistics	R	G	B
Roads	Minimum	44	59	72	Glass roofs	Minimum	69	107	135
	Maximum	210	223	246		Maximum	248	255	255
	Mean	118.34	146.77	164.64		Mean	166.21	201.80	228.31
	Std.dev	19.46	20.96	22.46		Std.dev	24.44	21.28	17.64
Grass	Minimum	34	52	30	Crop	Minimum	57	57	54
	Maximum	118	127	108		Maximum	174	167	154
	Mean	67.70	79.25	60.93		Mean	136.08	132.37	123.73
	Std.dev	13.09	10.51	10.82		Std.dev	10.48	9.91	9.52
Ground	Minimum	49	64	58	Grey buildings	Minimum	25	43	65
	Maximum	168	166	167		Maximum	116	154	194
	Mean	109.31	111.05	104.57		Mean	62.37	83.55	111.61
	Std.dev	17.89	15.67	15.66		Std.dev	10.10	12.04	11.83
No leaf Trees	Minimum	53	53	51	Forest	Minimum	21	32	43
	Maximum	187	187	190		Maximum	147	158	171
	Mean	96.85	92.52	91.53		Mean	73.21	76.02	81.33
	Std.dev	12.60	10.85	10.61		Std.dev	12.58	12.50	12.36
Bushes	Minimum	30	34	36	High grass	Minimum	54	63	58
	Maximum	108	99	106		Maximum	163	163	157
	Mean	56.71	46.37	49.41		Mean	109.48	112.54	108.98
	Std.dev	13.43	7.88	7.58		Std.dev	14.57	14.06	14.65
Red buildings	Minimum	69	43	42					
	Maximum	220	162	149					
	Mean	145.54	100.70	101.63					
	Std.dev	26.80	16.89	12.21					

In order to illustrate relations between classes, some scatter plots were generated (Fig. 20). According to the main rule of validation, scatter plots shouldn't have multiple clusters and the more separated are dots from different classes, the better. The first graph, which presents the correlation between Red and Grey buildings could serve as an example of well-created samples. Only small amount of pixels overlap and two groups are clearly separated.

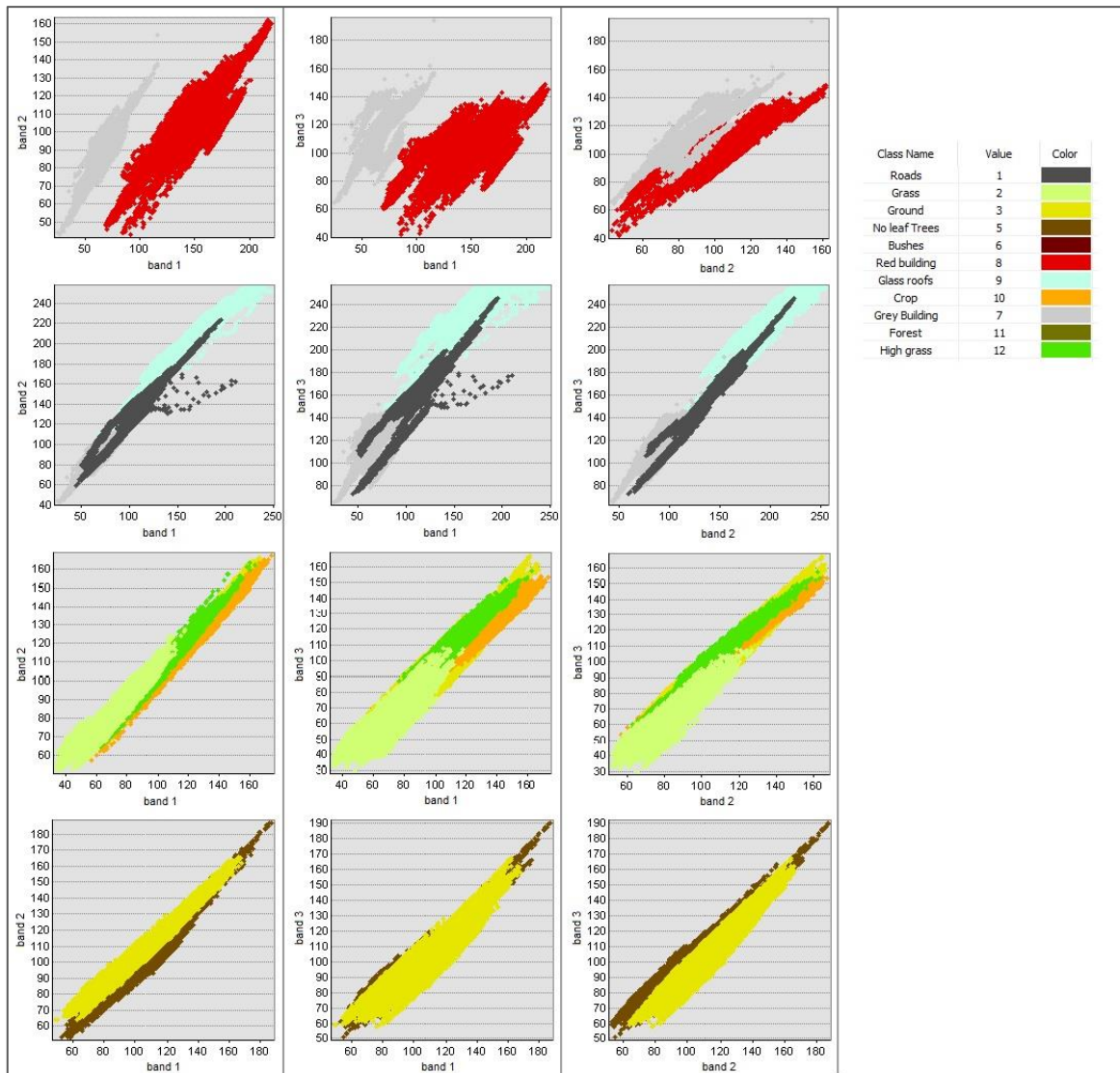


Figure 20 Training samples comparison with the use of Scatter Plots

On the second graph, one can see a relation between Roads, Grey buildings and Glass roofs. Glass roofs are located on the upper part of the graph, while Grey buildings at the bottom. As it is seen, the Road is placed in the middle, between them. Even though some pixels lie over pixels from different categories, classes could be regarded as distinct groups of pixels. As it was mentioned before, few classes representing ground have similar characteristics. The third graph illustrates their strong dependence. Grass, Crop and High grass classes are very close to each other and completely cover Ground class which is displayed in the background. However, it is not a big concern as the classes would be merged together in following steps in one extensive group. What would be a challenge in classification process is demonstrated on the last graph. There was no possibility to provide better distinction between Ground and No-leaf Trees categories. As the trees are not covered

by leaves and grass is not green yet, the features have almost the same spectral characteristics. Nevertheless, an attempt to perform classification with the use of eleven described training samples was carried out.

Four classifiers available in ArcGIS Pro software have been tested in order to assess their efficiency while classifying orthophotomap. Three of them: Support Vector Machines, Random Trees, and Maximum Likelihood required previously created training samples to perform supervised classification, while ISO Cluster algorithm generated cluster in process of unsupervised classification. Even though the workflow in ArcGIS Pro is quite straightforward, procedures needed to be supervised by the user, who was responsible for specifying classification parameters.

The essential parameter in Support Vector Machine algorithm is *Maximum Number of Samples per Class*. Since the default value 500, is recommended for nonsegmented rasters, the author decided to change the value. Setting value equal to zero resulted in using all the samples from the training sites to train the classifier. Maximum Likelihood algorithm doesn't require any additional parameters to specify so the process was launched as it was. On the contrary, while using Random Trees classifier, three input values are required: *Maximum Number of Trees*, *Maximum Tree Depth* and *Maximum Number of Samples per Class*. The higher first two values, the better accuracy could be obtained. Depending on visual assessment, values 50 – 30 – 0 seemed to give sufficient accuracy. Increasing the number of first two parameters didn't change the results at all. While completing ISO cluster classification, in order to provide a comparison with the three previous algorithms, *Minimum Number of Clusters* was set to be 11. Rest of the possible to specify parameters was set as default: *20 Iterations of Clustering Process*, *5 Cluster Merges per Iteration*, *0.5 as Maximum Merge Distance*, *30 as Minimum Cluster Size*, *10 as Skip Factor*. Different modifications of listed parameters didn't cause any visible changes in output raster.

3.4.3 Accuracy assessment

First, the results were assessed visually. Attached Figure 21 illustrates four classified rasters which are an output of classification process. Even though all of them have many imperfections, one can detect single features and get an overview of study area appearance. As it might have been suspected, the worst outcome was produced by ISO Classifier. Lack of training samples in unsupervised classification led to grouping pixels in meaningful classes. It was mainly due to the fact that picture scenery had many pixels with similar spectral

characteristics and there were only a few obvious classes such as Red building, Glass roof or Road. Pixels classified as a ground incorrectly covered areas referring to parking or buildings roofs and classes were not smooth. Also, Maximum Likelihood algorithm didn't result in satisfying classified raster. The main problem was salt and pepper effect present on the whole image area. Surprisingly, Crop class was very wide and faultily covered areas of buildings, roads, and parking.

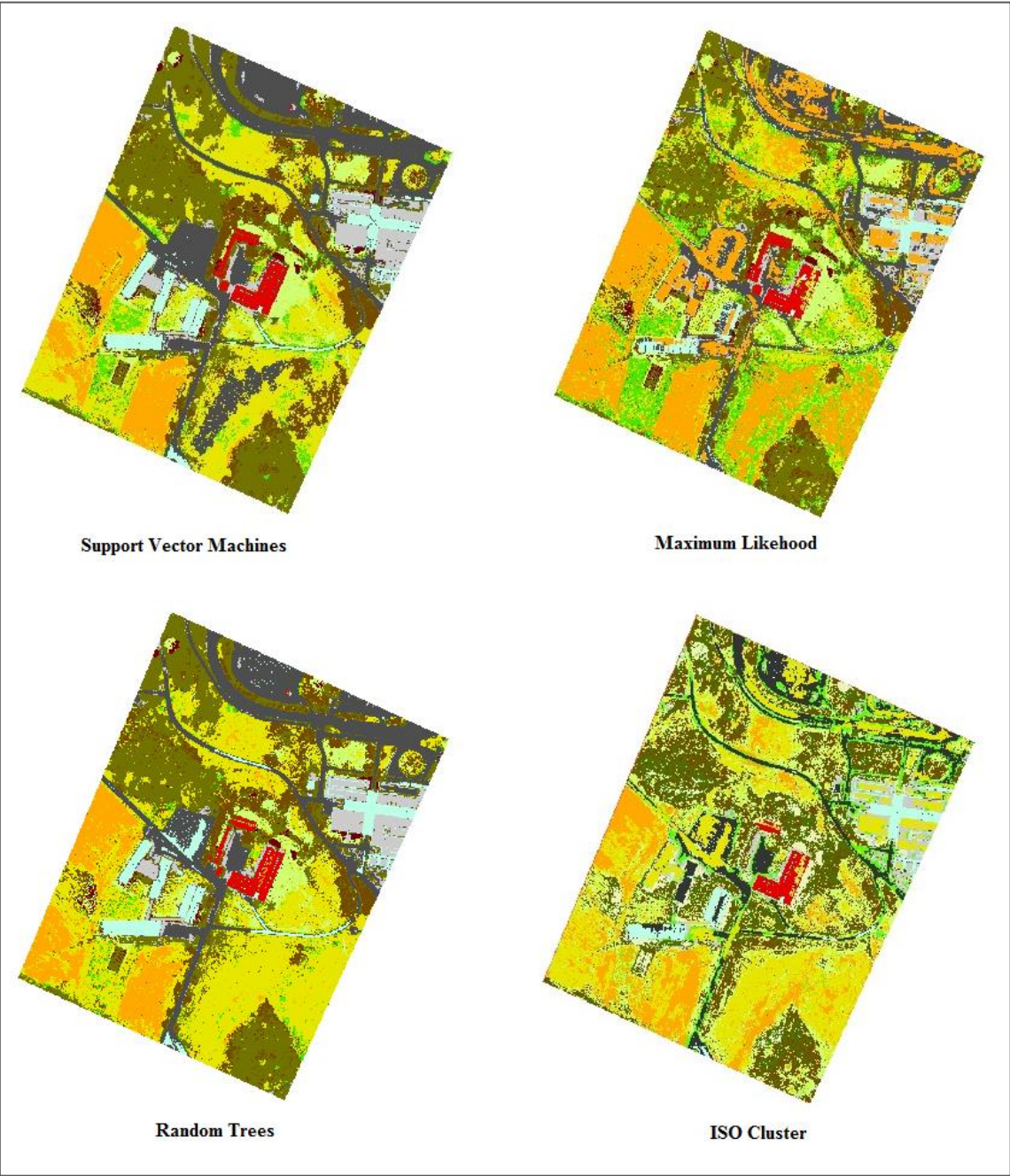


Figure 21 Image classification results

At a glance, SVM and RT seemed to derive similar outputs. In comparison to ML, classes are smoother and more clumped. There were few places where Road was misclassified with Glass buildings but it was is not a fault of the classifier as when one could look at the original orthophoto in some parts of the image sunlight had made road unusually bright. All the buildings were classified in a similar way but SVM seemed to be more precise while presenting Red buildings class. Also, Forest and No leaf Trees categories distribution was comparable on both rasters. The main difference is the bottom right corner, which should be covered by forest surrounded by bare earth. While RT output raster reminds the ground truth to a great extent, the SVM output raster resulted in Road and No leaf Trees classes wrongly assigned to this area.

Since visual judgment is very subjective, statistical evaluation was carried out. To provide the assessment with the use of statistics, the confusion matrices for three rasters were computed. Due to the fact, that ISO Cluster algorithm's output didn't produce satisfying results, clusters weren't merged into the classes, so the raster was excluded from confusion matrix computations.

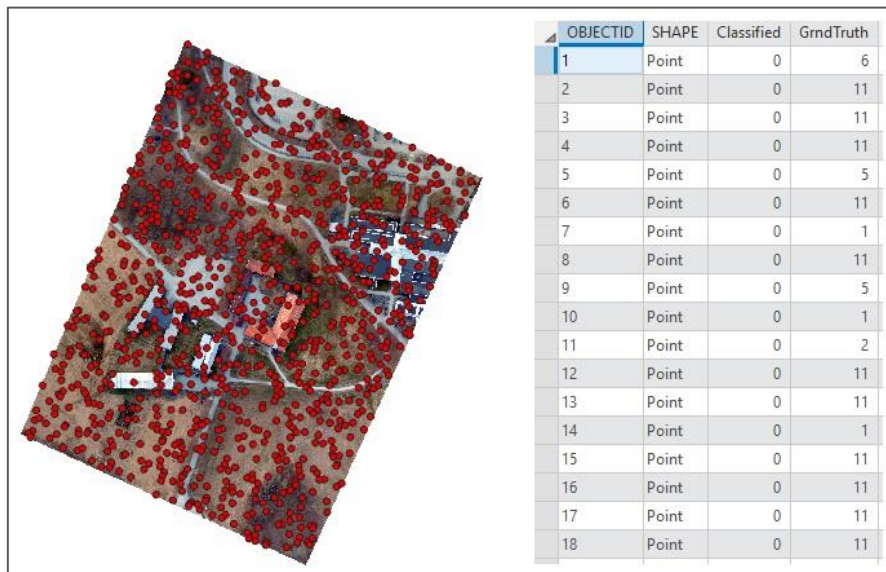


Figure 22 Reference dataset with its attribute table

As the reference dataset, the feature layer with one thousand points representing ground truth was adopted (Fig. 22). Information about real nature of the features was acquired from analyzing orthophotomap combined with a knowledge of the study area. According to recommendations from ArcGIS documentation, an optimal number of points for reliable accuracy assessment is $10*n$ for one class, where n is a number of classes. Having eleven land

cover categories, there should be 110 points for one class, which gives 1210 points in total. Due to the fact, that few classes were going to be merged before final assessment, 1000 points were regarded as sufficient number. Points were randomly distributed within each class, where each class had a number of points proportional to its relative area. Regarding point layer's attribute table, *GrndTruth* column was filled by the author, while *Classified* column was completed in *Update Accuracy Assesment Points* process and varies depending on analyzed raster.

Table 8 Confusion Matrix for Support Vector Machine classifier

Class	C_1	C_2	C_3	C_5	C_6	C_7	C_8	C_9	C_10	C_11	C_12	Total	U_Acc	Kappa
C_1	152	0	25	0	0	4	0	6	0	1	0	188	0.81	
C_2	0	38	5	2	0	0	0	0	0	1	0	46	0.83	
C_3	0	16	169	14	0	0	0	0	12	7	10	228	0.74	
C_5	0	5	37	49	0	0	1	0	6	9	1	108	0.45	
C_6	1	0	1	1	5	0	0	0	0	1	0	9	0.56	
C_7	10	0	0	0	0	35	0	0	0	0	0	45	0.78	
C_8	0	0	0	0	0	0	14	0	0	0	0	14	1.00	
C_9	8	0	0	0	0	1	0	30	0	0	0	39	0.77	
C_10	0	0	26	1	0	0	0	0	65	0	0	92	0.71	
C_11	15	1	32	12	4	3	3	0	0	129	3	202	0.64	
C_12	1	1	18	1	0	0	0	0	0	1	7	29	0.24	
Total	187	61	313	80	9	43	18	36	83	149	21	1000	0.00	
P_Acc	0.81	0.62	0.54	0.61	0.56	0.81	0.78	0.83	0.78	0.87	0.33	0.00		
Kappa														0.63

Table 9 Confusion Matrix for Maximum Likelihood classifier

Class	C_1	C_2	C_3	C_5	C_6	C_7	C_8	C_9	C_10	C_11	C_12	Total	U_Acc	Kappa
C_1	101	0	3	0	0	6	0	6	0	0	0	116	0.87	
C_2	0	47	11	0	0	0	0	0	1	1	0	60	0.78	
C_3	1	8	111	22	1	0	2	0	3	18	7	173	0.64	
C_5	0	3	18	41	0	1	0	0	5	19	1	88	0.47	
C_6	0	0	1	0	6	0	0	0	0	2	0	9	0.67	
C_7	14	0	1	0	0	18	0	0	0	0	0	33	0.55	
C_8	0	0	0	0	0	2	12	0	0	0	0	14	0.86	
C_9	6	0	0	0	0	2	1	23	0	0	0	32	0.72	
C_10	52	0	89	5	0	13	0	7	72	2	1	241	0.30	
C_11	13	1	15	6	2	1	3	0	0	98	2	141	0.70	
C_12	0	2	64	6	0	0	0	0	2	9	10	93	0.11	
Total	187	61	313	80	9	43	18	36	83	149	21	1000	0.00	
P_Acc	0.54	0.77	0.35	0.51	0.67	0.42	0.67	0.64	0.87	0.66	0.48	0.00		
Kappa														0.47

Table 10 Confusion Matrix for Random Trees classifier

Class	C_1	C_2	C_3	C_5	C_6	C_7	C_8	C_9	C_10	C_11	C_12	Total	U_Acc	Kappa
C_1	148	0	1	0	0	3	0	3	0	0	0	155	0.95	
C_2	0	46	2	0	0	0	0	0	0	2	0	50	0.92	
C_3	1	9	241	18	0	0	0	0	0	5	13	287	0.84	
C_5	0	0	27	57	0	0	2	0	6	1	2	95	0.60	
C_6	1	0	0	2	7	0	0	0	0	0	0	10	0.70	
C_7	10	0	0	0	0	35	0	0	0	0	0	45	0.78	
C_8	0	0	0	1	0	0	12	0	0	0	0	13	0.92	
C_9	13	0	0	0	0	0	0	33	0	0	0	46	0.72	
C_10	0	0	4	0	0	0	0	0	77	0	0	81	0.95	
C_11	14	6	28	2	2	5	4	0	0	140	2	203	0.69	
C_12	0	0	10	0	0	0	0	0	0	1	4	15	0.27	
Total	187	61	313	80	9	43	18	36	83	149	21	1000	0.00	
P_Acc	0.79	0.75	0.77	0.71	0.78	0.81	0.67	0.92	0.93	0.94	0.19	0.00		
Kappa														0.76

Confusion matrices for three classification methods were presented in the tables above (Tab. 8, 9 and 10). Columns and rows symbolize reference and classified data respectively. As it was mentioned before, the classes are as follows: Roads (1), Grass (2), Ground (3), No leaf Trees (5), Bushes (6), Grey buildings (7), Red buildings (8), Glass roofs (9), Crop (10), Forest (11) and High grass (12). User accuracy (U_Acc) stands for commission error, while Producer accuracy (P_Acc) is referred to errors of omission. The total column shows the number of points that should have been identified as a given class according to the reference data, while total row shows the number of points that were identified as a given class, according to the classified map. Considering *Kappa* parameter as the main indicator of classification accuracy the most satisfactory results were obtained by RT classifier (76%), the next was SVM classifier (63%) and the least accurate was ML classifier (47%). Nevertheless, there are some other conclusions which could be formulated based on confusion matrix computations. First of them is poor classification quality of High grass class for all methods resulting in user accuracy equal to 0.24 for SVM, 0.11 for ML and 0.27 for RT. Creating the class might have not been a good idea as it didn't have any special spectral characteristics but was used more as a support for classifying ground pixels. What is more, the name for this category had also been chosen incorrectly, as after verification in the field it occurred to be typical grass but with unusual color which was lying on the ground. Analyzing tables, the problem with distinction Ground form No leaf Trees occurred for all three classifiers. The worst are commission and omission errors for No leaf Trees class (0.45 and 0.61 for SVM,

0.47 and 0.51 for ML, 0.60 and 0.71 for RT), but confusion with ground pixels, influenced also Ground class errors significantly (0.74 and 0.54 for SVM, 0.64 and 0.35 for ML, 0.84 and 0.77 for RT). Regarding incorrect classification of bottom right corner of the map by SVM classifier, 25 out of 188 pixels from reference set were assigned to Road category, while they were a ground. It doesn't seem to be a lot, but as spectral characteristics for Road and Ground class are completely different in theory, it indicates an error in the classification process. For RT's confusion matrix both omission and commission errors values for all the categories despite High grass are comparable, which imply that any of class is an outlier.

As the Random Trees algorithm outweighs other classification methods both visually and based on statistics, it was adopted for further analyses. Some manual corrections were carried out to improve the content of the classes. It mainly came down to removing the Glass roof category from roads and parking, indicating the surface of red buildings, changing Grass category into Forest, in places where green trees were present and removing Ground category from forested areas. More important was to remove ground classes from areas where non-ground object were presented than in the opposite. Secondly, to clarify uncertainties among different categories of ground, Ground, Grass, Crop and High grass classes were merged into one group. Analogous, No leaf Trees class was combined with Forest class. Both reference dataset and classified raster were reclassified, which resulted in 6 classes: Roads (1), Grey buildings (7), Red buildings (8), Glass roofs (9), Forested areas (13), Ground (14) (Fig. 23d).

Table 11 Final Confusion Matrix

Class	C_1	C_7	C_8	C_9	C_13	C_14	Total	U_Acc	Kappa
C_1	161	3	0	3	0	1	168	0.96	
C_7	10	36	0	0	0	0	46	0.78	
C_8	0	0	16	1	1	0	18	0.89	
C_9	2	0	0	32	0	0	34	0.94	
C_13	13	4	2	0	226	72	317	0.71	
C_14	1	0	0	0	11	405	417	0.97	
Total	187	43	18	36	238	478	1000	0.00	
P_Acc	0.86	0.84	0.89	0.89	0.95	0.85	0.00		
Kappa									0.82

The confusion matrix was computed once again in order to validate the effectiveness of undertaken solutions (Tab. 11). *Kappa* parameter value increased significantly, from 76% to 82%. A quick check was done to ensure what was *Kappa* value after manual improvement but

before merging classes. The value occurred to be 78% which means that 4% of accuracy change was dependent on the correlation between classes corresponding to one land cover category such as ground and forested areas. In the 6th row and 7th column, value 72 which is out of diagonal probably stands for difficulties in distinguishing between Ground and No leaf Trees. However, the author considered acquired accuracy as sufficient in terms of implementing classified raster in further analysis. As the final step of the classification process, the raster was reclassified into ground and non-ground classes by assigning attribute values 1 and 0 respectively. In order to present results, raster was converted into polygon and clipped with original orthophotomap. Figure 23 illustrates the whole process of image classification.

3.4.4 Post-classification processing

Following objective of the workflow was to exclude all non-ground features from point cloud with respect to classified raster. It might have been accomplished by clipping the raster with point cloud generated in Agisoft PhotoScan. The challenge to process datasets with different dimension appeared. After some research and investigations, the author decided to implement non-commercial LAStools software. It is a collection of tools used for managing point clouds. Even though the software package is dedicated for LiDAR data, it is capable of performing analyses on all datasets in .las format. However, to perform clipping operation, raster had to be converted into polygon which covered only ground areas. To avoid loss of information, raster was converted without simplifying polygons method. It took more time but the layer was converted into exactly the same shape as it was for the raster. Next, LAStools was launched and the output was classified point cloud in .las format.

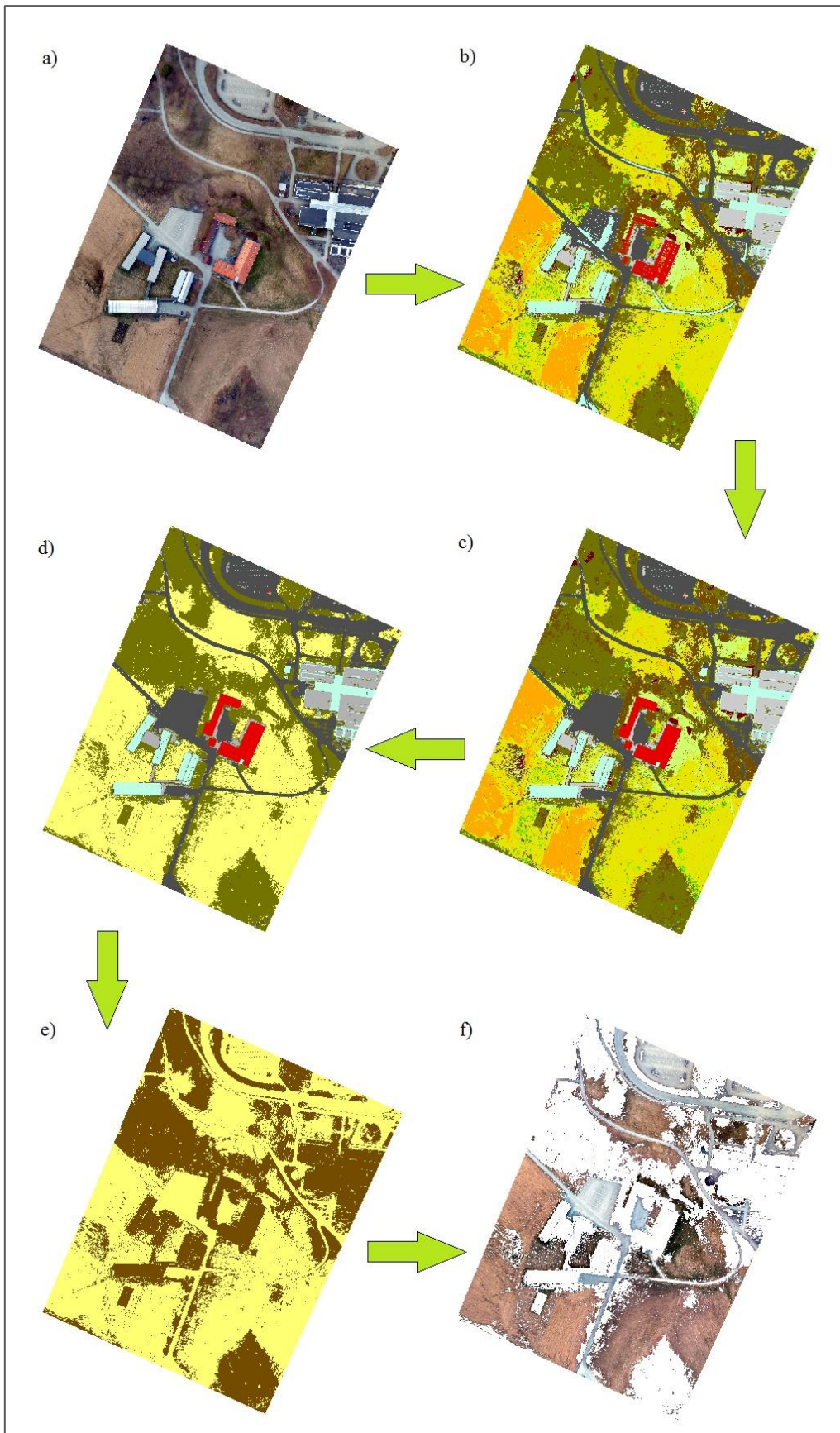


Figure 23 Classification process: a) Original orthophotomap b) RT Supervised classification c) Manual corrections d) Reclassification e) Reclassification in ground and non-ground f) Clipped orthophotomap

3.5 DEM generation

Producing Digital Elevation Models was the last step of the process. In order to provide a comparison between two methods of classification, two DEMs from two different point clouds in the .las format were going to be generated in ArcGIS Pro with the use of the same parameters. First point cloud was the output from Agisoft PhotoScan (chapter 3.3.4). With the use of software algorithms, point cloud classification had been done, and ground class which contained all points which cover bare earth surface was exported from the software. The second point cloud was generated by the author in a procedure of image classification completed with clipping point cloud with classified raster. One may ask, why to generate DEM for point cloud from Agisoft PhotoScan if it had already been generated? Using this DEM in comparison would not depict differences in classification approaches. As algorithms to create DEM used in Agisoft PhotoScan and ArcGIS Pro are different, two outputs would vary not only because of the classification approach but also because of various DEM generation parameters. Thus, the model was produced in one software in order to eliminate the impact of the later one.

To compare two point clouds not only visually, they need to be processed and converted into another product. The tool implemented in ArcGIS Pro *LAS dataset to raster* allows converting point cloud into Digital Elevation Model. Parameters possible to specify are: *Interpolation Type*, *Output Data Type*, *Sampling Type* and *Z Factor*. Interpolation technique is used to determine cell values of the output raster. Two methods are available: *binning* and *triangulation*. *Binning* approach provides Cell Assignment Method for determining each output cell using the points that fall within its extent, along with a Void Fill Method to determine the value of cells that do not contain any LAS points. The *Triangulation* interpolation methods derive cell values using a TIN based approach and this one was chosen for DEM generation. As a triangulation method, *Natural Neighbors* was adopted instead of *Linear* technique. An output data type was set to be *Float*, which resulted in 32-bit floating point raster. To define the resolution of output raster *Cellsize* was chosen as the method of *Sampling Type*. The cell size was set to be 5 cm. *Z factor* is generally used to convert Z linear units to match XY linear units. As the coordinate system of the project was established at the beginning, there was no need to change elevation values and multiply them by any unit.

The tool was run twice and two rasters were generated (Fig. 24).

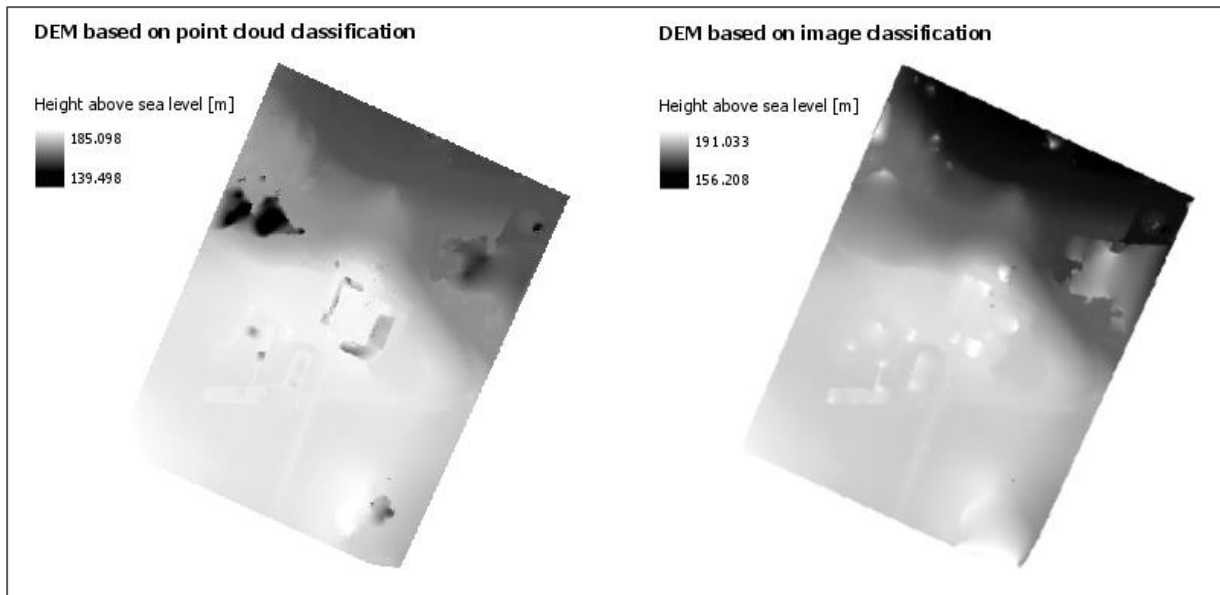


Figure 24 DEMs generated in ArcGIS Pro

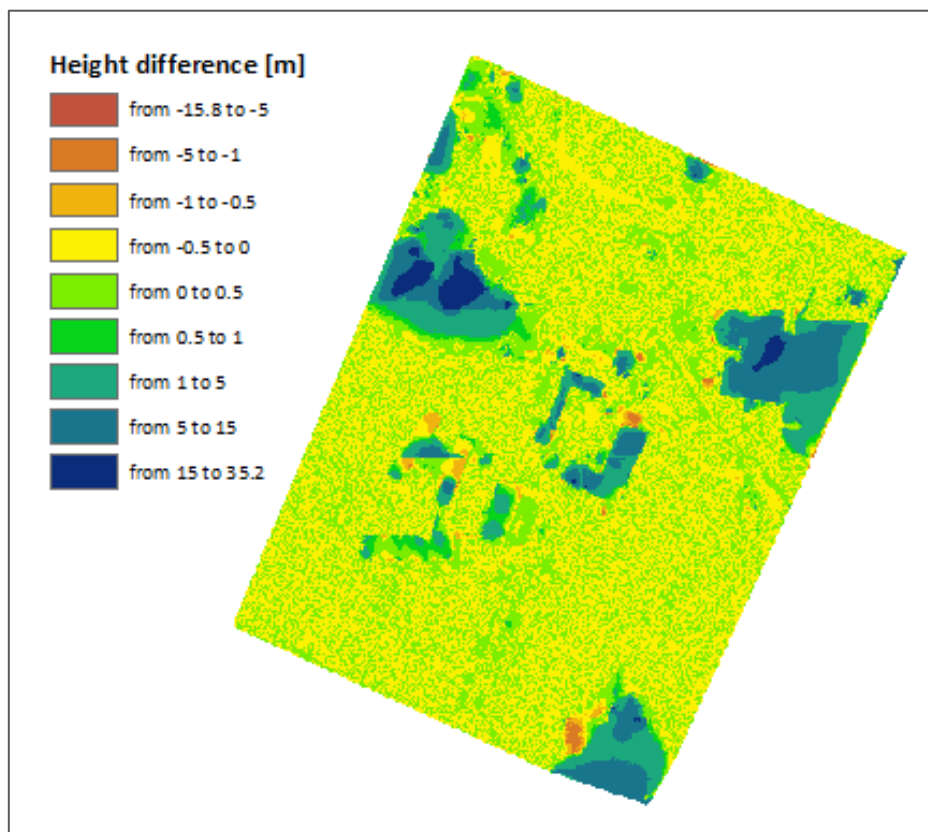


Figure 25 Elevation difference between two DEMs

By visual assessment, the models vary significantly. Both contain some failures, especially in the areas under the buildings so it is rather subjective to declare which of them performs better. However, DEM generated from point cloud classified in Agisoft PhotoScan

seems to have more distinct outliers. An example are black holes on the left part of the study area. They indicate the lowest elevation on the map while they cover the forested area in reality. All the mistakes contribute to the differences in minimum and maximum values of rasters. The minimum value for raster from classification in Agisoft is 139.5, while for raster which is the result of image classification it is 156.2. Maximum values are 185.1 and 191.0 respectively. In order to provide a comparison based on numerical values, map algebra functions were implemented to subtract rasters and depict differences among the whole study area. DEM based on point cloud classification was subtracted from DEM based on image classification. An outcome of the operation was raster illustrating deviations in elevation between two rasters. Different colors were assigned to manually created intervals. As it is presented on the figure 25, for a substantial part of the study area the difference between rasters is smaller than 0.5 m. Raster values vary the most under the buildings and forests. The dark blue color indicates values greater than 15 meters, which means that on the DEM from point cloud classification, the objects are situated much lower than on the DEM from image classification. ArcScene program was adopted to visually recognize the reason for outliers on the map. Two classified point clouds were imported into the software and displayed with RGB values in 3D view (Fig. 26).

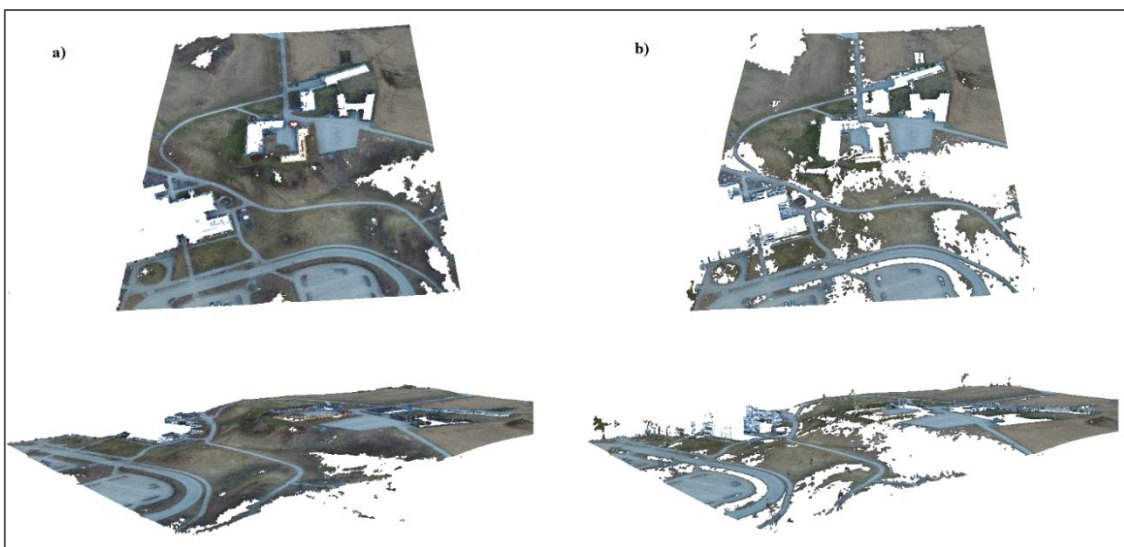


Figure 26 Classified point cloud: a) point cloud classification b) image classification

At a glance, point cloud created based on image classification seems to have many holes and small isolated regions of points. Nevertheless, the white spaces indicate places where there are buildings, trees, and bushes, which were not detected by Agisoft PhotoScan

algorithm while classifying point cloud. Also, the isolated islands of points are there on purpose, as they present ground for example surrounded by trees but some of its parts are visible on the photos. Thus, the fact that point cloud from Agisoft looks smoother and neater, does not mean that it is better for generating DEM. What is more, areas comprising trees, which were not excluded from the point cloud affect the process of generating DEM, as algorithm regards these points for bare earth, which would result in a false model generation.

After analysing classified cloud points in 3D view, the reasons for outliers on the models were found. Point cloud from Agisoft contains a lot of points which are below the ground level (Fig. 26). These are the blunders which were created during image matching while processing raw images from a drone. They might have been deleted manually in early steps of the whole workflow. As they weren't, it implies that classifying algorithm implemented in Agisoft PhotoScan was not capable of detecting them. These points are mainly distributed under buildings and forested areas, so because there are other points in these regions, Digital Elevation Model is adjusted to them and causes the erroneous surface of bare earth. Also, the lower part of most of the buildings was regarded by the algorithm as the ground and it explains the darker color of these areas on model (Fig. 24). On the other side, there is a model created based on image classification. As it was mentioned before, white holes are not the problem as most of them cover forested regions or single trees. And even though some of the holes mask bare earth areas, it should not be a concern, as triangulation algorithm is capable of interpolating these surfaces. Nevertheless, the complication occurred in the proximity of buildings as some of their edges were classified as Ground class during image classification. It was probably due to imperfections in orthophotomap content as the boundaries of buildings were not very clear and their spectral characteristics might have been regarded as a wrong class. As these outstanding pixels are not distributed evenly, the results are diverse colors corresponding to the buildings on DEM (Fig. 24).

What wasn't noticed before, is the fact that some non-ground objects were not correctly reconstructed on the point cloud. Most single trees but also some small regions of high vegetation were presented as points of the ground surface. As the photos were captured in early spring, trees didn't have leaves, so their shape was only bough and branches. Together with a lack of oblique images, it may have affected the results of image matching. On the other hand, it exposed the weakness of products delivered by UAV photogrammetry.

For both DEMs, manual improvements of classified point cloud might had been performed before generation process. However, the author wanted to examine the potential of almost fully automated workflow with the use of two different approaches. One conclusion is

that points which are below the ground or points which present edges of the buildings could be easily deleted manually with no special workload. The difficulty appears while pixels are wrongly classified and cells which present non-ground objects are regarded by classification algorithm as bare-earth points and serve for DEM generation.

4 DISCUSSION AND CONCLUSIONS

The objective of the thesis was to examine image based classification approach and its effectiveness in generating Digital Elevation Models from drone imagery. All required stages of the workflow were accomplished and 5 cm resolution DEM was created. Any additional field measurements were carried out so the validation of the results is based on visual assessment, comparison of two different approaches and other observations related to the subject. As the project workflow was a complex process with many steps influencing the quality of final DEM, separate comments on each step are required. An overview of consecutive project's phases would help to define the relevance of proposed method.

Regarding technical issues related to image acquisition stage, one should have in mind that all the considerations are appropriate for the consumer-grade drone. Nevertheless, an outcome of image processing carried out in two different software packages brought a positive view on products derived from UAV photogrammetry. The overall accuracy of the bundle block adjustment expressed as RMS error on control points was 6.12 cm for Pix4D Mapper and 7.91 cm for Agisoft PhotoScan. There were also no complications while generating other products such as orthophotomaps, point clouds, and Digital Surface Models. What is more, it was demonstrated that despite different workflows, two software packages are capable of delivering comparable results. Even though the values were satisfying, the author found some possible improvements.

Applying a professional, survey dedicated drone would probably result in better resolution of orthophotomap and higher accuracies of bundle block adjustment. Main differences between two types of drones, which could affect acquired products, are camera optics, the accuracy of Inertial Measuring Unit and better stability of flight. Also, the method of Ground Control Points measurements had an impact on adjustment accuracy. Employing GNSS static technique instead of RTK GNSS method would deliver lower errors on GCPs coordinates. Moreover, better distribution of GCP with locating them closer to the edges of the study area could have been employed. According to the Agisoft Manual, the optimal number of GCP is 10, which means that solution implemented in the project does not fulfil software requirements. Increasing the number of GCP may improve adjustment accuracy, but on the other hand, the author considers it as pointless to establish ten Ground Control Points on the area which covers only 45 000 m². Undoubtedly, flight parameters are another element

to consider while analysing obtained results. It could be a separate subject of research to examine different options of flight and their influence on whole project's accuracy. Nevertheless, to summarize considerations in this section of the project, it can be stated that the process of image acquisition with the use of UAV photogrammetry was successfully completed together with post-processing of acquired images.

The most challenging was the succeeding stage of the project which deals with the complex process of image classification. Many problems considering the creation of classes, choice of appropriate training samples, specifying parameters of classifying algorithms and validation of results have already been described in section 3.4. As the image classification is commonly employed in satellite imagery, classifying high-resolution orthophotomap (GSD = 3.36 cm) occurred to be problematic part due to lack of corresponding literature. The classification was completed as a result of the iterative process by trial and error method. Selection of classes and their representative training samples turned out to be a crucial stage of the process. Due to fact that photos were captured early spring, colors of vegetation were almost identical for the entire area of study and distinction based on spectral characteristics of different vegetation types was very problematic. The conclusion is that creating smaller classes which represent pixels typical for an exact class is more effective than creating few extensive classes which contain many different pixels contributing to one category. In the later example, there is no clear distinction between classes, so the classifying algorithm needs to guess where to assign pixels.

In the project, it was also demonstrated that machine learning classification algorithms such as Support Vector Machines and Random Trees perform better classification results than classical methods like Maximum Likelihood or unsupervised classification ISO Cluster algorithm. The highest accuracy was obtained with the use of Random Trees classifier. *Kappa* parameter was originally 76% and after some manual improvements and merging corresponding classes, the value increased to 82%. In author opinion, the accuracy of classification could be higher if the camera mounted on a drone would have more spectral bands. Probably, one infrared band would be enough to improve the *Kappa* value significantly. Another consideration is lighting on images. Captured photos seemed to be a little bit dark due to the fact that the flight mission was performed in the evening. It had an impact on spectral characteristics of all the features of the study area as the colors were not very apparent. On the other hand, it allowed avoiding shadows covering study area. The compromise between these two factors depends on the individual survey and its application.

The main assumption of the classification process was that ground category covering non-ground objects was much more serious concern than in opposite way. It was due to the fact that all areas classified as non-ground features would be removed, so even if some parts of grass or road would be classified as non-ground objects, the interpolation algorithm implemented to generate DEM, will be capable of interpolating the empty surface in these areas. On the contrary, if the building was wrongly classified as a ground, the pixels within this area remain, so interpolation algorithm involves them while generating DEM.

In the last stage of the project workflow, DEM generation followed by DEMs comparison were accomplished. Two classified point clouds were processed in the same software with the use of the same parameters in order to provide a comparison among point clouds but not DEM generation algorithms. The concern introduced at the beginning of the thesis has been confirmed as the ground filtering algorithm in turned out to be ineffective. Due to fact that it was generated especially for LiDAR data, not all of the above-ground objects were removed correctly. Nevertheless, as some trees were not correctly reconstructed on the dense point cloud, the evaluation of classification performed in Agisoft PhotoScan was limited.

The aim of the thesis was to examine the potential of the image classification method and conclude if it could be a beneficial substitute for point cloud classification technique while generating DEM from UAV imagery. It was possible to produce DEM with the resolution of 5 cm. Its accuracy assessment was accomplished as a comparison with the model based on point cloud classification. In general, two models delivered comparable results. For a substantial part of the study area, the difference between models was smaller than 0.5 m, and the number and distribution of outliers was similar. However, the image based approach was capable of detecting more non-ground objects and misclassified regions did not affect interpolation significantly. The author also described some shortcomings of the process and suggested improvements which could be applied to enhance results of image classification. Having this in mind allows formulating the conclusion that the proposed approach has a big potential, however, it needs to be examined in broader research. One more confirmation of this statement is the fact that results of the whole project strongly depend on nature of the input data. By input data author means the quality of captured images mainly determined the by drone camera optics but also characteristics of the study area, comprising elevation changes and the presence of non-ground objects. All of these aspects contribute to the performance of the algorithms implemented in the process of image processing, image

classification, and DEM generation. That is why there is no unambiguous answer for the question which techniques and parameters are the most appropriate to use.

In conclusion, ground filtering is a challenging process when generating Digital Elevation Models. The specification of point cloud generated from images captured by the drone makes the process even more demanding. Two approaches were presented by the author, however, any one of them was capable of classifying point cloud with 100% success. It was proved that image classification method can bring results comparable to point cloud classification. Moreover, in some problematic regions, it outweighs the commonly used classification based on point cloud. In the author's opinion, there is a space for further improvements for both approaches. What could be suggested is a hybrid approach which could involve point cloud classification assisted by image based classification. As it was presented, the main problem of point cloud classification appears in areas close to the object above the earth surface such as trees or buildings. Algorithms implemented in software are not capable of performing accurate division between ground and non-ground class. Generally, lower parts of these objects are classified as a ground class which leads to erroneous DEM. As the boundaries between for example buildings and grass are usually clear on orthophotomap, the image classification algorithms could be implemented in areas where non-ground class abuts the ground. Nevertheless, an idea of combining two approaches seems to be a challenge as then, the algorithms would need to work simultaneously on two data sources which are dense point cloud and orthophotomap.

Bibliography

Agisoft LCC, 2016. *AgisoftPhotoscan User Manual, Version*

Akar, O., 2017. The rotation forest algorithm and object-based classification method for land use mapping through UAV images. *Geocarto International*.

Bhandari, B., Oli, U., Panta, N. & Pudasaini, U., 2015. *Generation of High Resolution DSM Using UAV Images*. Sofia, Bulgaria, FIG Working Week.

Bhatta, B., 2008. *Remote Sensing and GIS*. New Delhi: Oxford University Press.

DJI, 2015. *Phantom 3 Advanced - User Manual*..

Eisenbeib, H., 2009. *UAV Photogrammetry*, University of Technology Dresden.

Eisenbeiss, H., 2004. *A mini unmanned aerial vehicle (UAV): System overview and image acquisition*. Pitsanulok, Thailand,

ESRI Support, 2017. *ArcGIS Pro ESRI website support*. [Online]
Available at: <http://pro.arcgis.com/en/pro-app/>

Hengl, T. & Evans, I. S., 2009. Mathematical and Digital Models of Land Surface. *Developments in Soil Science*, pp. Chapter 2: 31-64.

Kraus, K., 2007. *Photogrammetry: Geometry from images and laser scans*. Berlin: Walter de Gruyter.

Liu, X., 2008. Airborne LiDAR for DEM generation: some critical issues. *Progress in Physical Geography*, pp. 31-49.

Madawalagama, S. L., Munasinghe, N., Dampegana, S. P. & Samarakoon, L., 2016. Low cost aerial mapping with consumer-grade drones. *Geoinformatics Centre, Asian Institute of Technology*.

Okamoto, J. & Shimazaki, H., 2015. Land surveying performance of commercially-available inexpensive small UAV. *Asian Assotiation on Remote Sensing*.

Pix4D, 2016. *Pix4D Mapper 3.1 User Manual*.

Polat, N. & Uysal, M., 2015. Investigating performance of Airborne LiDAR data filtering algorithms for DTM generation. *Mesurement*, pp. 61-68.

Remondino, F. et al., 2011. *UAV Photogrammetry for mapping and 3D modeling - curent status and future perspectives*. Zurich, Switzerland, International Archives of the Photogrammetry, Remote Sensing and Spatial Information Sciences.

Ruiz, J. J., Diaz-Mas, L., Perez, F. & Viguria, A., 2014. Evaluating the accuracy of DEM generation algorithms from UAV imagery. *Mapping*, pp. 38-45.

Sona, G. et al., 2014. Experimental analysis of different software packages for orientation and digital surface modelling from UAV images. *Earth Science Informatics*, pp. 97-107.

Uysal, M., Toprak, A. S. & Polat, N., 2015. DEM generation with UAV Photogrammetry and accuracy analysis in Sahitler hill. *Measurement*, pp. 539-543.

Weih, R. C. & Riggan, N. D., 2010. Object-based classification vs. pixel-based classification: comparative importance of multi-resolution imagery. *The International Archives of the Photogrammetry, Remote Sensing and Spatial Information Sciences*.

Wendel, J., Bittenfield, B. P. & Stanislawski, L. V., 2015. An evaluation of unsupervised and supervised learning algorithms for clustering landscape types in the US. *Cartography and Geographic Information Science*, 43(3), pp. 233-249.

Yilmaz, V. et al., 2016. Image classification-based ground filtering of point clouds extracted from UAV-based aerial photos. *Geocarto International*.

List of figures

Figure 1 Fixed wing eBee SenseFly, Rotary wing Mavic DJI.....	7
Figure 2 Drone Phantom 3 Advanced	11
Figure 3 Various surveying techniques for 3D recording purposes.....	12
Figure 4 Principle of bundle block adjustment.	15
Figure 5 Difference between DSM and DTM/DEM.....	16
Figure 6 Digital Terrain Model	17
Figure 7 TIN model and grid model.....	18
Figure 8 Supervised classification scheme.....	20
Figure 9 Unsupervised classification scheme	20
Figure 10 Study area with GCP and CP.....	28
Figure 11 Mission planning in Pix4D Capture.....	31
Figure 12 Manual measurements of control points in Agisoft and in Pix4D.....	36
Figure 13 Orthophotomap generated in Agisoft and in Pix4D	39
Figure 14 Blunders in classified point cloud.....	40
Figure 15 Digital Elevation Model generated in Agisoft and in Pix4D.....	40
Figure 16 Original orthophotomap and clipped orthophotomap.....	42
Figure 17 Segmentation process	43
Figure 18 Results of pre – classification	44
Figure 19 Training samples.....	45
Figure 20 Training samples comparison with the use of Scatter Plots	47
Figure 21 Image classification results	49
Figure 22 Reference dataset with its attribute table	50
Figure 23 Classification process	55
Figure 24 DEMs generated in ArcGIS Pro	57
Figure 25 Elevation difference between two DEMs	57
Figure 26 Classified point cloud	58

List of tables

Table 1 Phantom 3 Advanced specifications	10
Table 2 Features of aerial, close range and UAV photogrammetry	12
Table 3 Confusion matrix.....	24
Table 4 Measured Ground Control Points.....	29
Table 5 Processing results from Pix4D Mapper and Agisoft PhotoScan.....	38
Table 6 Statistics of original training samples	44
Table 7 Statistics of training samples	46
Table 8 Confusion Matrix for Support Vector Machine classifier.....	51
Table 9 Confusion Matrix for Maximum Likelihood classifier	51
Table 10 Confusion Matrix for Random Trees classifier.....	52
Table 11 Final Confusion Matrix	53

Appendices

Agisoft PhotoScan

Processing Report
06 May 2017



Survey Data

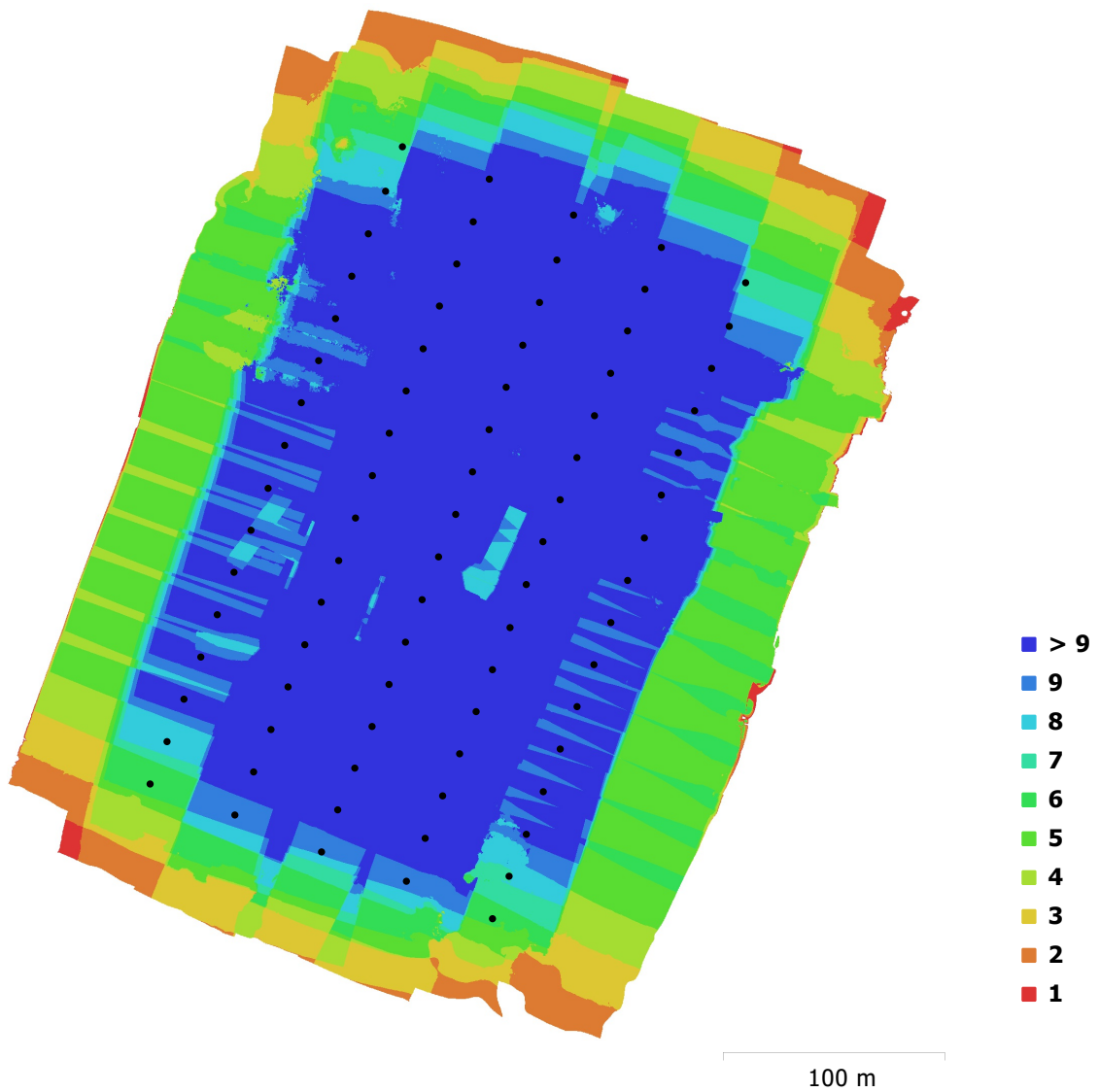


Fig. 1. Camera locations and image overlap.

Number of images:	80	Camera stations:	80
Flying altitude:	91.1 m	Tie points:	58,859
Ground resolution:	3.44 cm/pix	Projections:	314,517
Coverage area:	0.123 km ²	Reprojection error:	0.769 pix

Camera Model	Resolution	Focal Length	Pixel Size	Precalibrated
FC300S (3.61 mm)	4000 x 3000	3.61 mm	1.56 x 1.56 μm	No

Table 1. Cameras.

Camera Calibration

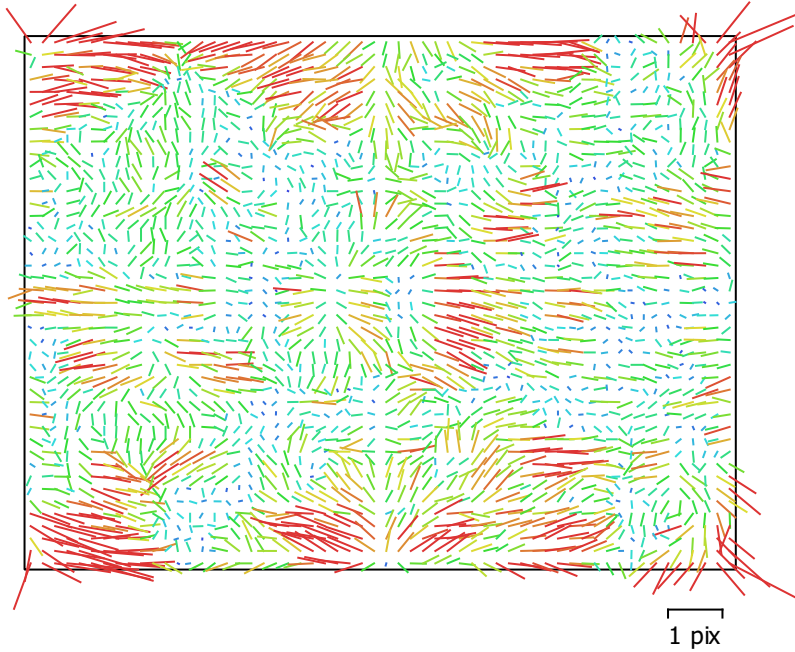


Fig. 2. Image residuals for FC300S (3.61 mm).

FC300S (3.61 mm)

80 images

Type
Frame

Resolution
4000 x 3000

Focal Length
3.61 mm

Pixel Size
1.56 x 1.56 μm

	Value	Error	F	Cx	Cy	K1	K2	K3	P1	P2
B1	-1.69597									
B2	0.139043									
F	2276.54	1.2	1.00	-0.52	-0.81	-0.59	0.43	0.05	-0.10	0.08
Cx	11.8044	0.05		1.00	0.41	0.31	-0.22	-0.03	0.34	-0.03
Cy	2.50859	0.071			1.00	0.47	-0.33	-0.06	0.10	0.09
K1	-0.0179743	4.8e-05				1.00	-0.91	0.66	0.05	-0.08
K2	0.0151774	8.2e-05					1.00	-0.87	-0.05	0.02
K3	0.00177358	4.4e-05						1.00	0.00	0.01
P1	-0.000604108	3.2e-06							1.00	0.02
P2	3.68009e-05	2.6e-06								1.00

Table 2. Calibration coefficients and correlation matrix.

Ground Control Points

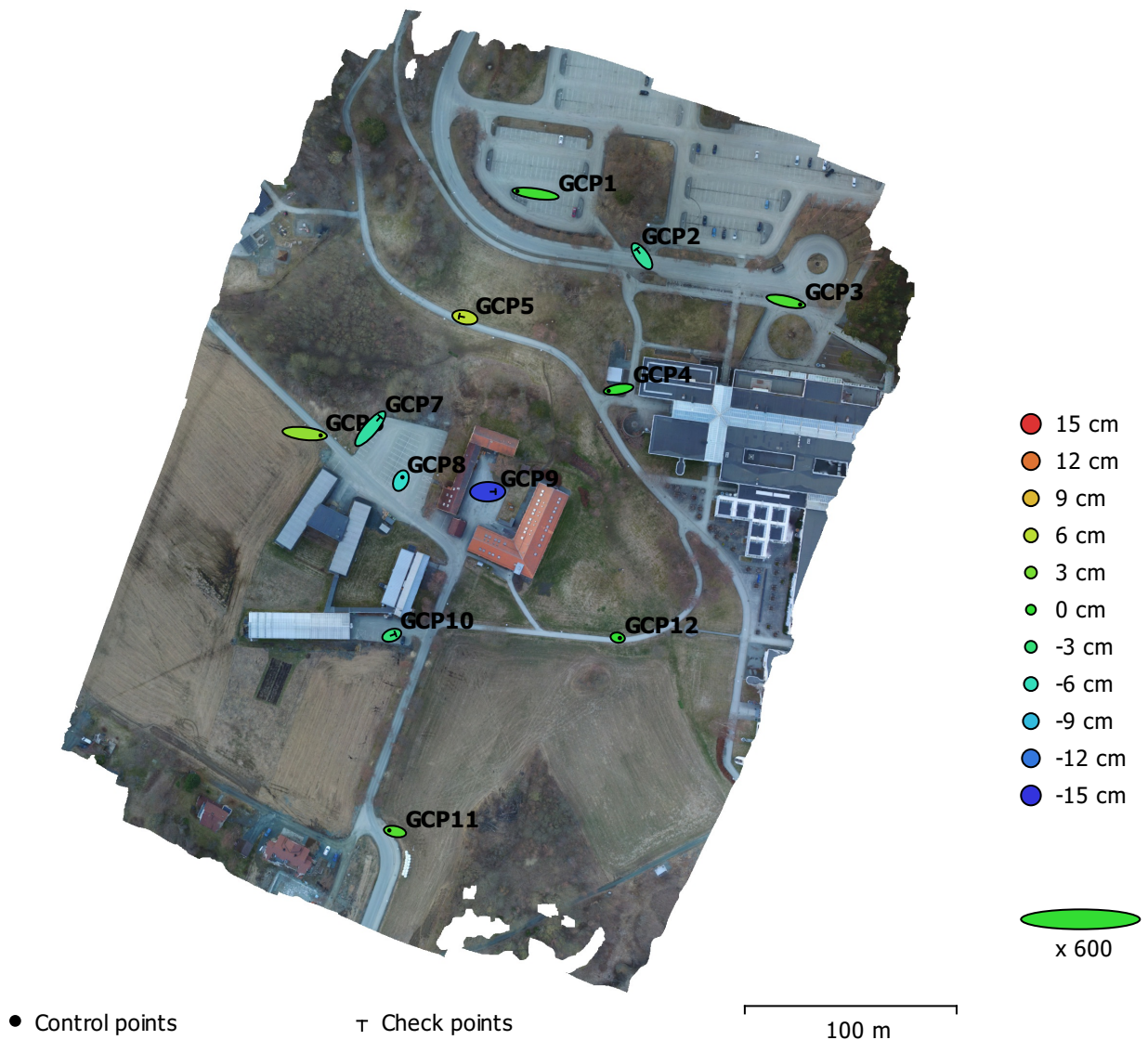


Fig. 3. GCP locations and error estimates.

Z error is represented by ellipse color. X,Y errors are represented by ellipse shape.

Estimated GCP locations are marked with a dot or crossing.

Count	X error (cm)	Y error (cm)	Z error (cm)	XY error (cm)	Total (cm)
7	1.80506	0.35264	3.06394	1.83919	3.57356

Table 3. Control points RMSE.

X - Easting, Y - Northing, Z - Altitude.

Count	X error (cm)	Y error (cm)	Z error (cm)	XY error (cm)	Total (cm)
5	1.08428	0.986819	7.77824	1.46611	7.9152

Table 4. Check points RMSE.

X - Easting, Y - Northing, Z - Altitude.

Label	X error (cm)	Y error (cm)	Z error (cm)	Total (cm)	Image (pix)
GCP1	-2.85001	0.406058	0.476114	2.9179	0.351 (14)
GCP11	-0.899542	0.181546	1.42964	1.69882	0.432 (8)
GCP12	0.341218	-0.0715446	-0.181716	0.393152	0.404 (10)
GCP3	2.23601	-0.494821	1.04115	2.51567	0.296 (8)
GCP4	-1.55358	-0.258706	-0.068103	1.57644	0.368 (14)
GCP6	2.50775	-0.284506	4.09318	4.80873	0.396 (10)
GCP8	0.239646	0.524218	-6.75038	6.77494	0.458 (15)
Total	1.80506	0.35264	3.06394	3.57356	0.393

Table 5. Control points.
X - Easting, Y - Northing, Z - Altitude.

Label	X error (cm)	Y error (cm)	Z error (cm)	Total (cm)	Image (pix)
GCP10	0.575601	0.214218	-3.08766	3.14815	0.270 (18)
GCP2	-0.819793	1.14133	-4.67991	4.88633	0.346 (16)
GCP5	-0.905035	0.187513	5.93006	6.00165	0.385 (17)
GCP7	1.58565	1.86681	-4.98859	5.55746	0.373 (14)
GCP9	1.24159	0.0196844	-14.5265	14.5794	0.451 (15)
Total	1.08428	0.986819	7.77824	7.9152	0.366

Table 6. Check points.
X - Easting, Y - Northing, Z - Altitude.

Digital Elevation Model

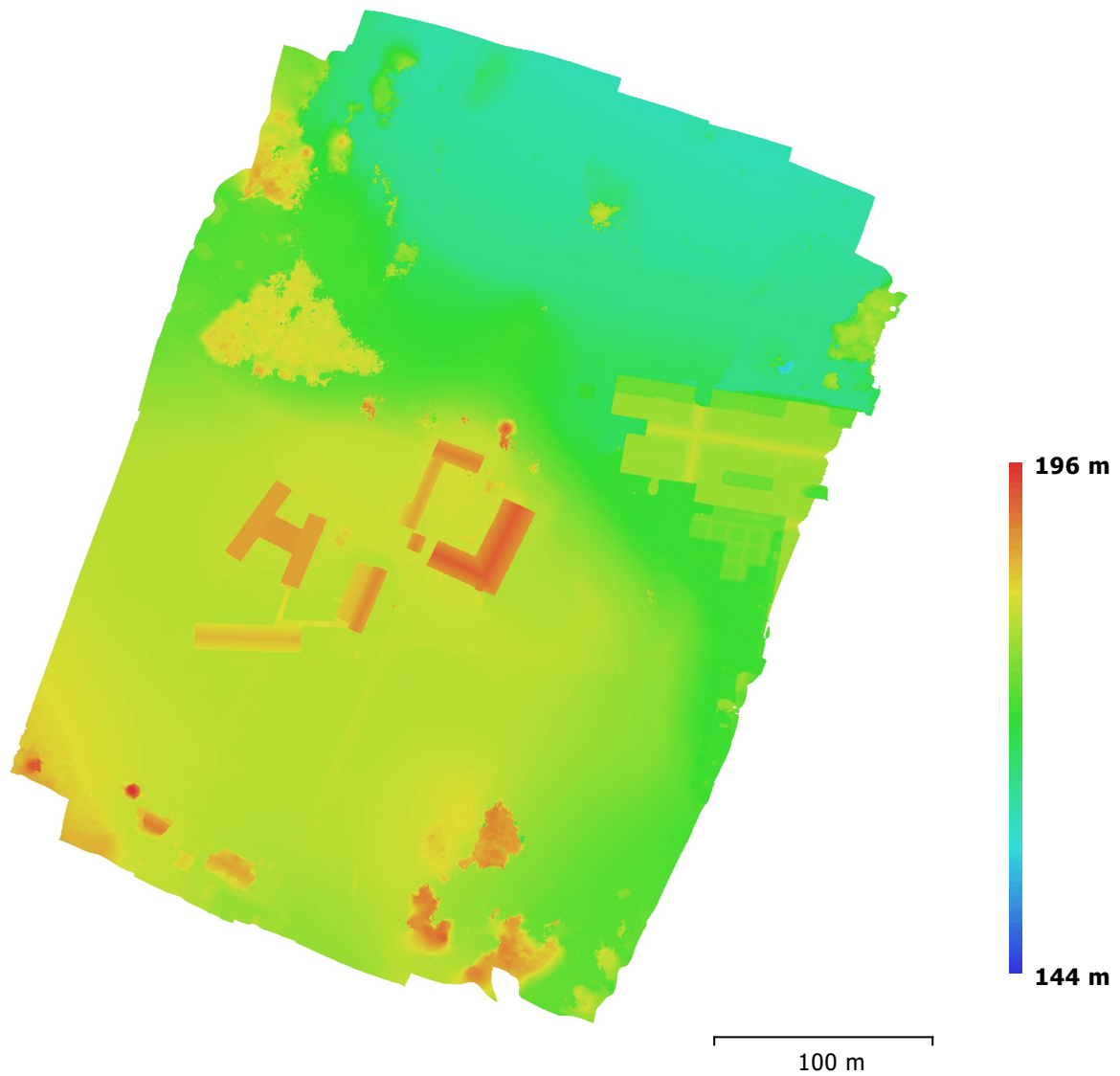


Fig. 4. Reconstructed digital elevation model.

Resolution: 6.88 cm/pix
Point density: 211 points/m²

Processing Parameters

General

Cameras	80
Aligned cameras	80
Markers	12
Coordinate system	ETRS89 / UTM zone 32N (EPSG::25832)
Rotation angles	Yaw, Pitch, Roll

Point Cloud

Points	58,859 of 62,311
RMS reprojection error	0.233851 (0.768706 pix)
Max reprojection error	1.04645 (23.9543 pix)
Mean key point size	3.46374 pix
Effective overlap	5.45849

Alignment parameters

Accuracy	High
Generic preselection	Yes
Reference preselection	Yes
Key point limit	40,000
Tie point limit	4,000
Adaptive camera model fitting	Yes
Matching time	5 minutes 49 seconds
Alignment time	10 seconds

Optimization parameters

Parameters	f, cx, cy, k1-k3, p1, p2
Fit rolling shutter	No
Optimization time	0 seconds

Dense Point Cloud

Points	28,902,841
--------	------------

Reconstruction parameters

Quality	High
Depth filtering	Moderate
Depth maps generation time	1 hours 49 minutes
Dense cloud generation time	3 minutes 30 seconds

Model

Faces	1,926,855
Vertices	968,922

Reconstruction parameters

Surface type	Arbitrary
Source data	Dense
Interpolation	Enabled
Quality	High
Depth filtering	Moderate
Face count	1,926,856
Processing time	32 minutes 15 seconds

DEM

Size	8,655 x 9,508
Coordinate system	ETRS89 / UTM zone 32N (EPSG::25832)

Reconstruction parameters

Source data	Dense cloud
Interpolation	Enabled
Processing time	1 minutes 27 seconds

Orthomosaic

Size	11,760 x 13,593
Coordinate system	ETRS89 / UTM zone 32N (EPSG::25832)
Channels	3, uint8

Reconstruction parameters

Blending mode	Mosaic
---------------	--------

Surface
Enable color correction
Enable hole filling
Processing time

Software

Version
Platform

Mesh
No
Yes
2 minutes 27 seconds

1.3.1 build 4030
Windows 64



Important: Click on the different icons for:



Help to analyze the results in the Quality Report



Additional information about the sections



Click [here](#) for additional tips to analyze the Quality Report

Summary



Project	ola_final
Processed	2017-05-05 23:34:26
Camera Model Name(s)	FC300S_3.6_4000x3000 (RGB)
Average Ground Sampling Distance (GSD)	3.36 cm / 1.32 in
Area Covered	0.1155 km ² / 11.548 ha / 0.0446 sq. mi. / 28.5505 acres
Time for Initial Processing (without report)	07m:03s

Quality Check



Images	median of 25664 keypoints per image	
Dataset	80 out of 80 images calibrated (100%), all images enabled	
Camera Optimization	0.05% relative difference between initial and optimized internal camera parameters	
Matching	median of 11558 matches per calibrated image	
Georeferencing	yes, 7 GCPs (7 3D), mean RMS error = 0.02 m	

Preview

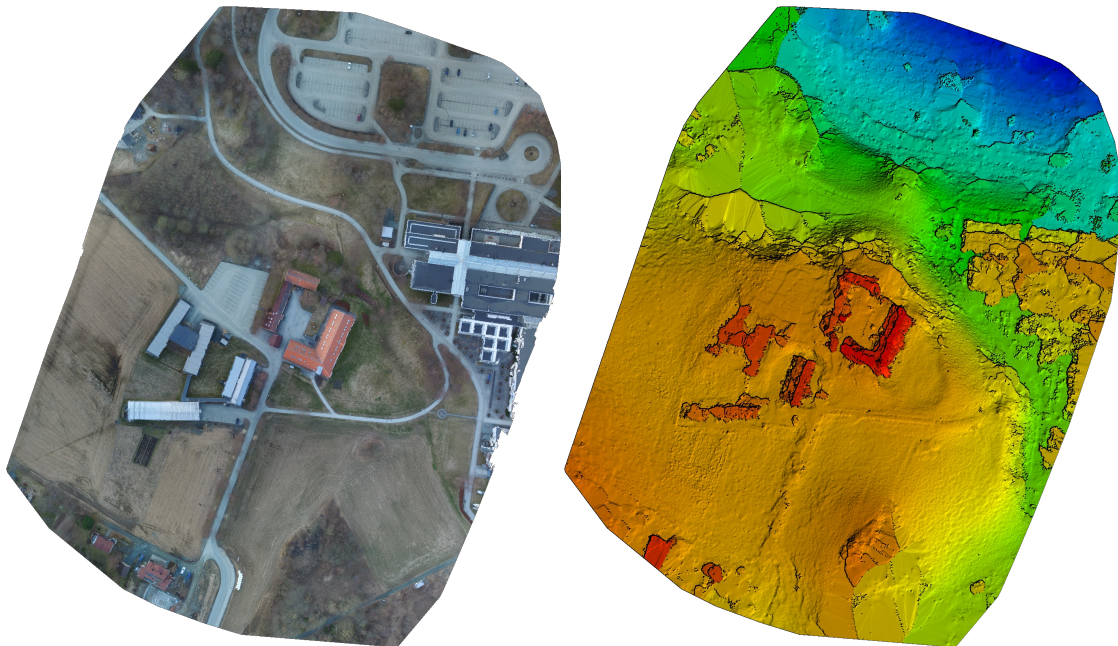


Figure 1: Orthomosaic and the corresponding sparse Digital Surface Model (DSM) before densification.

Calibration Details



Number of Calibrated Images	80 out of 80
Number of Geolocated Images	80 out of 80

Initial Image Positions

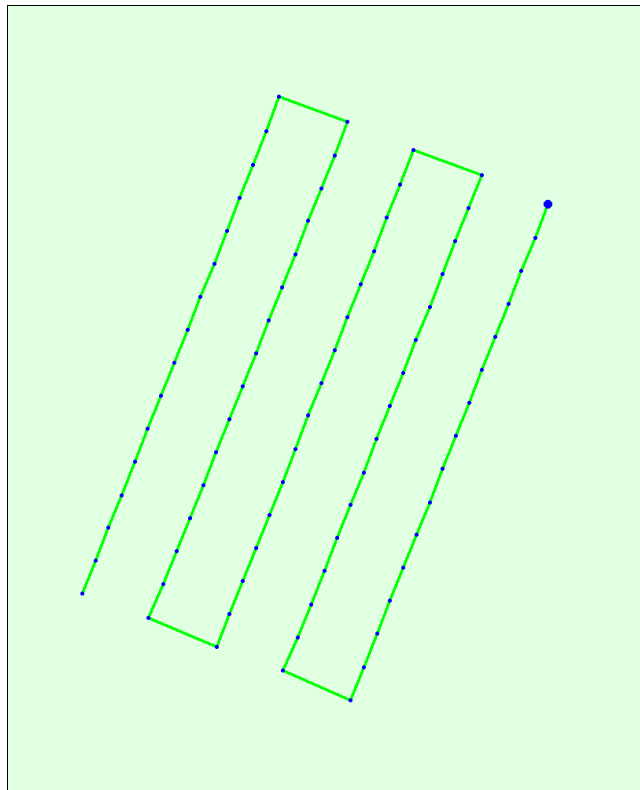
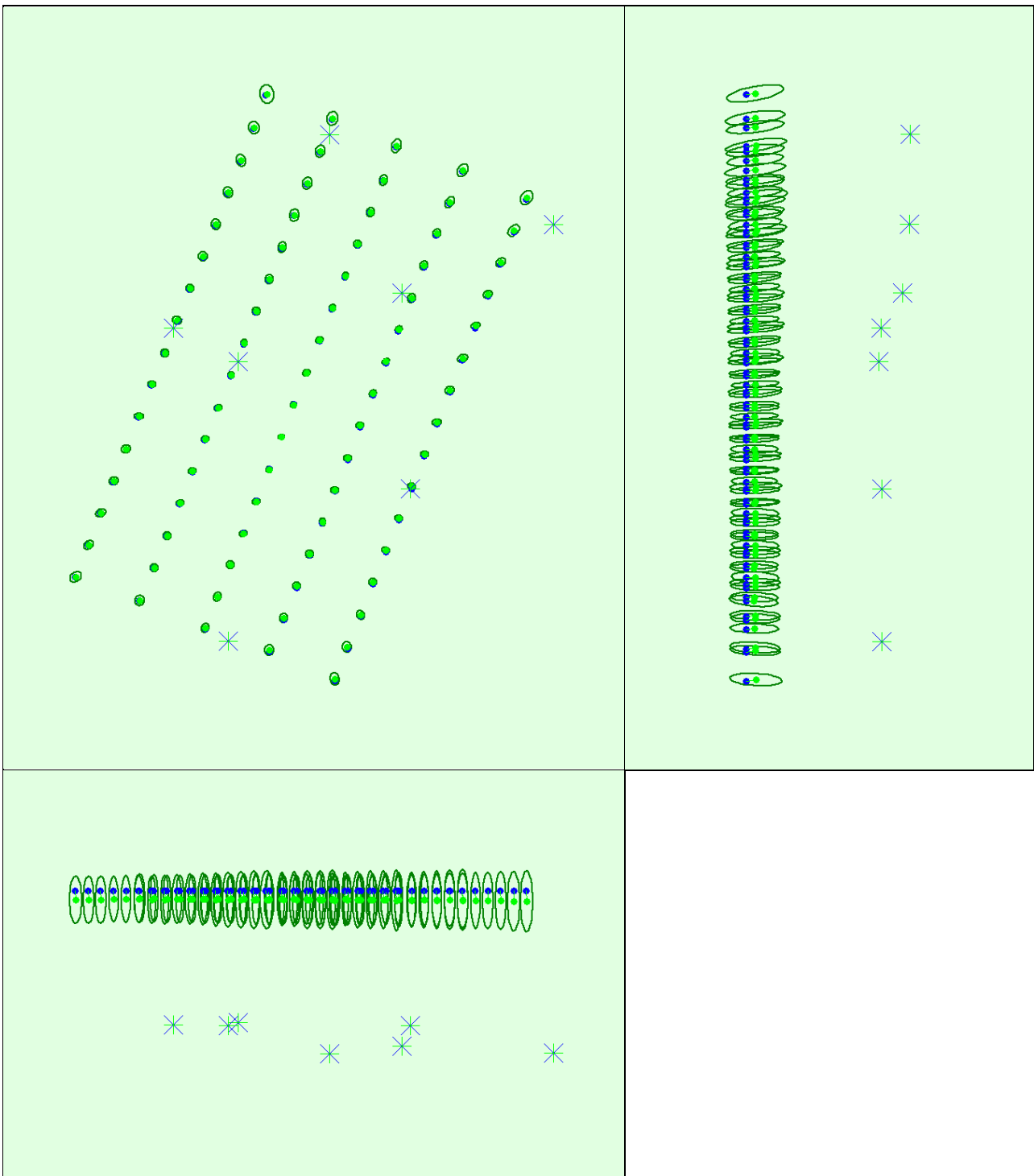


Figure 2: Top view of the initial image position. The green line follows the position of the images in time starting from the large blue dot.

Computed Image/GCPs/Manual Tie Points Positions





Uncertainty ellipses 100x magnified

Figure 3: Offset between initial (blue dots) and computed (green dots) image positions as well as the offset between the GCPs initial positions (blue crosses) and their computed positions (green crosses) in the top-view (XY plane), front-view (XZ plane), and side-view (YZ plane). Dark green ellipses indicate the absolute position uncertainty of the bundle block adjustment result.

? Absolute camera position and orientation uncertainties



	X[m]	Y[m]	Z[m]	Omega [degree]	Phi [degree]	Kappa [degree]
Mean	0.026	0.027	0.155	0.017	0.014	0.005
Sigma	0.005	0.007	0.012	0.004	0.003	0.001

? Overlap



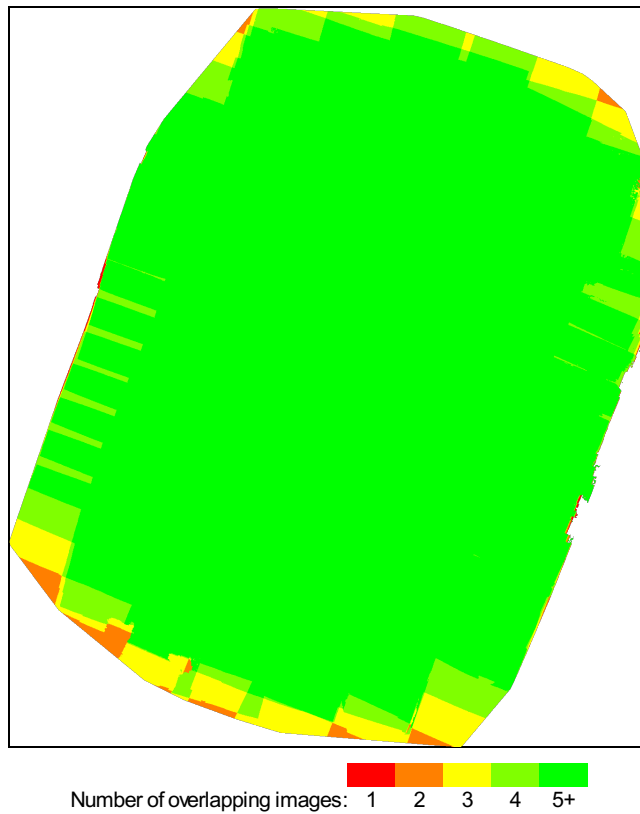


Figure 4: Number of overlapping images computed for each pixel of the orthomosaic. Red and yellow areas indicate low overlap for which poor results may be generated. Green areas indicate an overlap of over 5 images for every pixel. Good quality results will be generated as long as the number of keypoint matches is also sufficient for these areas (see Figure 5 for keypoint matches).

Bundle Block Adjustment Details

Number of 2D Keypoint Observations for Bundle Block Adjustment	935570
Number of 3D Points for Bundle Block Adjustment	275923
Mean Reprojection Error [pixels]	0.173

Internal Camera Parameters

FC300S_3.6_4000x3000 (RGB). Sensor Dimensions: 6.317 [mm] x 4.738 [mm]

EXIF ID: FC300S_3.6_4000x3000

	Focal Length	Principal Point x	Principal Point y	R1	R2	R3	T1	T2
Initial Values	2285.722 [pixel] 3.610 [mm]	2000.006 [pixel] 3.159 [mm]	1500.003 [pixel] 2.369 [mm]	-0.132	0.111	-0.016	0.000	0.000
Optimized Values	2284.423 [pixel] 3.608 [mm]	2010.768 [pixel] 3.176 [mm]	1501.645 [pixel] 2.372 [mm]	-0.018	0.016	0.002	0.000	-0.001
Uncertainties (Sigma)	4.458 [pixel] 0.007 [mm]	0.349 [pixel] 0.001 [mm]	0.340 [pixel] 0.001 [mm]	0.000	0.001	0.000	0.000	0.000

The number of Automatic Tie Points (ATPs) per pixel, averaged over all images of the camera model, is color coded between black and white. White indicates that, on average, more than 16 ATPs have been extracted at the pixel location. Black indicates that, on average, 0 ATPs have been extracted at the pixel location. Click on the image to see the average direction and magnitude of the re-projection error for each pixel. Note that the vectors are scaled for better visualization.

2D Keypoints Table

	Number of 2D Keypoints per Image	Number of Matched 2D Keypoints per Image
Median	25664	11558
Min	20106	4415
Max	32786	18440
Mean	25408	11695

🔍 3D Points from 2D Keypoint Matches



	Number of 3D Points Observed
In 2 Images	152763
In 3 Images	47768
In 4 Images	24131
In 5 Images	15213
In 6 Images	8915
In 7 Images	6230
In 8 Images	5210
In 9 Images	4491
In 10 Images	3442
In 11 Images	1971
In 12 Images	1654
In 13 Images	1497
In 14 Images	1326
In 15 Images	762
In 16 Images	222
In 17 Images	130
In 18 Images	75
In 19 Images	61
In 20 Images	35
In 21 Images	19
In 22 Images	6
In 23 Images	2

🔍 2D Keypoint Matches



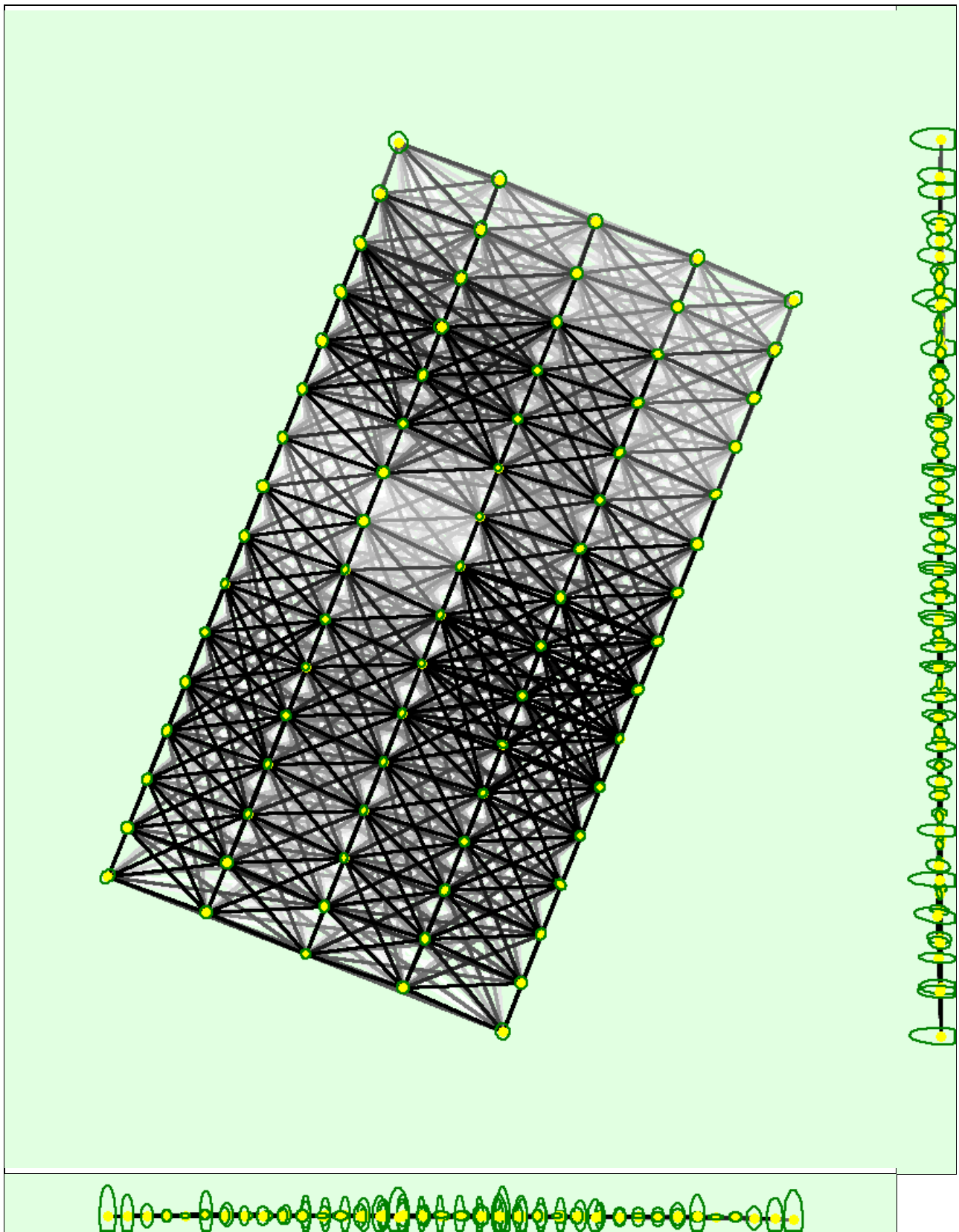


Figure 5: Computed image positions with links between matched images. The darkness of the links indicates the number of matched 2D keypoints between the images. Bright links indicate weak links and require manual tie points or more images. Dark green ellipses indicate the relative camera position uncertainty of the bundle block adjustment result.

? Relative camera position and orientation uncertainties



	X[m]	Y[m]	Z[m]	Omega [degree]	Phi [degree]	Kappa [degree]
Mean	0.021	0.023	0.046	0.060	0.039	0.007

Sigma	0.005	0.005	0.028	0.033	0.023	0.002
-------	-------	-------	-------	-------	-------	-------

Geolocation Details

Ground Control Points

GCP Name	Accuracy XY/Z [m]	Error X [m]	Error Y [m]	Error Z [m]	Projection Error [pixel]	Verified/Marked
GCP1 (3D)	0.020/ 0.020	-0.017	-0.024	0.009	0.665	14 / 14
GCP3 (3D)	0.020/ 0.020	0.028	-0.010	-0.017	1.012	8 / 8
GCP4 (3D)	0.020/ 0.020	0.020	-0.008	-0.010	1.003	15 / 15
GCP6 (3D)	0.020/ 0.020	-0.041	0.013	-0.033	0.824	10 / 10
GCP8 (3D)	0.020/ 0.020	-0.011	-0.003	0.015	0.923	15 / 15
GCP11 (3D)	0.020/ 0.020	0.000	0.031	0.018	0.649	7 / 7
GCP12 (3D)	0.020/ 0.020	0.034	0.003	-0.033	0.801	10 / 10
Mean [m]		0.002021	0.000400	-0.007203		
Sigma [m]		0.025077	0.016543	0.020176		
RMS Error [m]		0.025158	0.016548	0.021423		

0 out of 5 check points have been labeled as inaccurate.

Check Point Name	Accuracy XY/Z [m]	Error X [m]	Error Y [m]	Error Z [m]	Projection Error [pixel]	Verified/Marked
GCP2	0.0200/0.0200	-0.0052	-0.0222	0.0390	0.8129	16 / 16
GCP5	0.0200/0.0200	-0.0228	-0.0252	-0.0576	0.6288	17 / 17
GCP7	0.0200/0.0200	-0.0332	-0.0268	0.0130	0.7042	14 / 14
GCP9	0.0200/0.0200	-0.0215	0.0059	0.0910	1.0001	15 / 15
GCP10	0.0200/0.0200	-0.0126	0.0261	-0.0215	0.7020	18 / 18
Mean [m]		-0.019047	-0.008427	0.012799		
Sigma [m]		0.009551	0.021018	0.050859		
RMS Error [m]		0.021308	0.022645	0.052445		

Localisation accuracy per GCP and mean errors in the three coordinate directions. The last column counts the number of calibrated images where the GCP has been automatically verified vs. manually marked.

Absolute Geolocation Variance

Min Error [m]	Max Error [m]	Geolocation Error X [%]	Geolocation Error Y [%]	Geolocation Error Z [%]
-	-15.00	0.00	0.00	0.00
-15.00	-12.00	0.00	0.00	0.00
-12.00	-9.00	0.00	0.00	0.00
-9.00	-6.00	0.00	0.00	0.00
-6.00	-3.00	0.00	0.00	0.00
-3.00	0.00	52.50	43.75	56.25
0.00	3.00	47.50	56.25	43.75
3.00	6.00	0.00	0.00	0.00
6.00	9.00	0.00	0.00	0.00
9.00	12.00	0.00	0.00	0.00
12.00	15.00	0.00	0.00	0.00
15.00	-	0.00	0.00	0.00
Mean [m]		-0.267009	-0.500791	5.206821
Sigma [m]		0.171745	0.365407	0.323249
RMS Error [m]		0.317475	0.619931	5.216846

Min Error and Max Error represent geolocation error intervals between -1.5 and 1.5 times the maximum accuracy of all the images. Columns X, Y, Z show the percentage of images with geolocation errors within the predefined error intervals. The geolocation error is the difference between the initial and computed image positions. Note that the image geolocation errors do not correspond to the accuracy of the observed 3D points.

Geolocation Bias	X	Y	Z
Translation [m]	-0.267009	-0.500791	5.206821

Bias between image initial and computed geolocation given in output coordinate system.

Relative Geolocation Variance

Relative Geolocation Error	Images X [%]	Images Y [%]	Images Z [%]
[-1.00, 1.00]	100.00	100.00	100.00
[-2.00, 2.00]	100.00	100.00	100.00
[-3.00, 3.00]	100.00	100.00	100.00
Mean of Geolocation Accuracy [m]	5.000000	5.000000	10.000000
Sigma of Geolocation Accuracy [m]	0.000000	0.000000	0.000000

Images X, Y, Z represent the percentage of images with a relative geolocation error in X, Y, Z.

Geolocation Orientational Variance	RMS [degree]
Omega	1.476
Phi	0.275
Kappa	2.142

Geolocation RMS error of the orientation angles given by the difference between the initial and computed image orientation angles.

Initial Processing Details

System Information

Hardware	CPU: Intel(R) Xeon(R) CPU E5-2670 v2 @ 2.50GHz RAM: 32GB GPU: NVDIA Quadro K5000 (Driver: 10.18.13.5362)
Operating System	Windows 10 Education, 64-bit

Coordinate Systems

Image Coordinate System	WGS84 (egm96)
Ground Control Point (GCP) Coordinate System	ETRS89 / UTM zone 32N (egm96)
Output Coordinate System	ETRS89 / UTM zone 32N (egm96)

Processing Options

Detected Template	No Template Available
Keypoints Image Scale	Full, Image Scale: 1
Advanced: Matching Image Pairs	Aerial Grid or Corridor
Advanced: Matching Strategy	Use Geometrically Verified Matching: no
Advanced: Keypoint Extraction	Targeted Number of Keypoints: Automatic
Advanced: Calibration	Calibration Method: Standard Internal Parameters Optimization: All External Parameters Optimization: All Rematch: Auto, yes Bundle Adjustment: Classic

Point Cloud Densification details

Processing Options

Image Scale	multiscale, 1/2 (Half image size, Default)
Point Density	Optimal
Minimum Number of Matches	3
3D Textured Mesh Generation	yes
3D Textured Mesh Settings:	Resolution: Medium Resolution (default) Color Balancing: no
Advanced: 3D Textured Mesh Settings	Sample Density Divider: 1
Advanced: Matching Window Size	7x7 pixels
Advanced: Image Groups	group1
Advanced: Use Processing Area	yes
Advanced: Use Annotations	yes
Advanced: Limit Camera Depth Automatically	no
Time for Point Cloud Densification	03m:22s
Time for 3D Textured Mesh Generation	05m:20s

Results



Number of Generated Tiles	1
Number of 3D Densified Points	6030009
Average Density (per m ³)	78.26

DSM, Orthomosaic and Index Details



Processing Options



DSM and Orthomosaic Resolution	1 x GSD (3.37 [cm/pixel])
DSM Filters	Noise Filtering: yes Surface Smoothing: yes, Type: Sharp
Raster DSM	Generated: yes Method: Inverse Distance Weighting Merge Tiles: yes
Orthomosaic	Generated: yes Merge Tiles: yes GeoTIFF Without Transparency: no Google Maps Tiles and KML: no
Raster DTM	Generated: yes Merge Tiles: yes
DTM Resolution	5 x GSD (3.37 [cm/pixel])
Time for DSM Generation	12m:19s
Time for Orthomosaic Generation	08m:59s
Time for DTM Generation	06m: